Multi-scale EO-based agricultural drought monitoring indicator for operative irrigation networks management in Italy

Chiara Corbari, Nicola Paciolla, Giada Restuccia, Al Bitar Ahmad

Journal of Hydrology: Regional Studies 52 (2024) 101732

Contents lists available at ScienceDirect

Journal of Hydrology: Regional Studies

journal homepage: www.elsevier.com/locate/ejrh

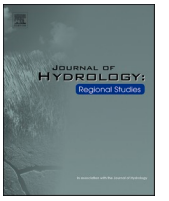

Multi-scale EO-based agricultural drought monitoring indicator for operative irrigation networks management in Italy

Chiara Corbari [a,*], Nicola Paciolla [a], Giada Restuccia [a], Ahmad Al Bitar [b]

[a] Politecnico di Milano, Piazza Leonardo da Vinci 32, Milan 20133, Italy
[b] CESBIO (Université de Toulouse, CNES, CNRS, IRD), Toulouse, France

ARTICLE INFO

Keywords:
Agricultural drought
Multi satellites data
Irrigation volumes
Crop yield

ABSTRACT

Study region: Two irrigation Consortia in Italy: the Chiese in Lombardia Region and the Capitanata in Puglia Region.
Study focus: Drought monitoring is crucial especially where the rainfall regime is irregular and agriculture is mainly based on irrigated crops, such as in Mediterranean countries. In this work, the main objective is to develop an EO-based agricultural drought monitoring indicator (ADMIN) for operative irrigation networks management. The ADMIN indicator considers different levels of drought conditions combining anomalies of rainfall, soil moisture, land surface temperature and vegetation indices. Multiple remote sensing data, which differ on sensing techniques, spatial and temporal resolutions and spectral bands, are used and the uncertainty in anomalies computation derived from the use of multiple sources of remote sensing datasets is also discussed. The analyses are performed for the two Irrigation Consortia, which differ for climate, irrigation volumes and techniques, and crop types.
New hydrological insights for the region: The obtained results show an inverse dependency between the cumulated ADMIN and the irrigation volumes in the Capitanata area (which has on-demand irrigation), whereas the dependency is much weaker in the Chiese Consortium (where irrigation is provided on a fixed basis, independently from the drought conditions). In both areas, the role of irrigation is critical to sustain production and preserve crop yields, which seem almost uncorrelated to ADMIN. ADMIN has demonstrated to outperform the use of single anomalies.

1. Introduction

Drought is an intensifying hazard with a complex behavior affecting both the natural and anthropogenic environments as well as the socio-economic activities (Sheffield, et al., 2009; Van Loon et al., 2014; Mann and Gleick, 2015; Wood et al., 2015; Douville et al., 2021; Seneviratne et al., 2021). According to the Munich Re report (Munich Re, 2021), between 2000 and 2019, the 35% of hazard events are related to droughts affecting more than 1.43 billion people: as the drought of 2003 in central Europe (García-Herrera et al., 2010) or of 2010 in Russia (Spinoni et al., 2018), the 2013–2014 California drought (Swain et al., 2014), the Chinese event of 2014 (Wang and He, 2015), the southern Africa drought of 2015–2017 (Meza et al., 2021), and the Australian 2000 event (van Dijk et al., 2013). In particular, strong negative impacts have been reported on the agricultural sector, with different effects depending on the crops being rainfed or irrigated, mainly due to water shortages with reductions of crop productions and consequently economic losses

* Corresponding author.
E-mail address: chiara.corbari@polimi.it (C. Corbari).

https://doi.org/10.1016/j.ejrh.2024.101732
Received 22 September 2023; Received in revised form 4 March 2024; Accepted 5 March 2024
Available online 8 March 2024

(De Stefano et al., 2015; Ding et al., 2011). These drought events are further projected to increase due to climate change and also increased land-atmosphere feedbacks due to changed land/vegetation coverage and also irrigated areas (Miralles et al., 2019). Thus, irrigated agriculture, which is by far the largest water user with about 70% of total freshwater consumption (Alexandratos and Bruinsma, 2012), will be more and more impacted, even though irrigated areas cover only about 2% of the global land area (FAO, 2016). Therefore, an improvement in the understanding of the spatial and temporal variability of droughts is required to meet the increasing effects of droughts (AghaKouchak et al., 2015).

Drought is generally defined as a temporal anomaly in comparison with average conditions over long time periods (Wood et al., 2015). Wilhite and Glantz (1985) identified four different types of droughts based on their impacts: i) meteorological as a precipitation deficiency, ii) agricultural as soil water availability shortage, iii) hydrological for low runoff and groundwater deficiency, iv) socio-economic on the society. Each type of drought might evolve with different timing, intensity, duration and spatial extent (Vicente-Serrano, 2006). To describe this complex phenomenon, a huge number of drought indices has been developed over the years, designed for different applications. However, no single drought index has been identified to describe the multifaceted nature of drought (Wanders et al., 2017). Therefore, the World Meteorological Organization (WMO) and Global Water Partnership (GWP) (2016) suggest to use multiple drought indices.

Among them, the Standardized Precipitation Index (SPI) is defined by the WMO as the standard index for analysing a meteorological drought (World Meteorological Organization, 2012), by fitting the precipitation data to a standardized normal probability distribution function, over different time scales from 1 to 36 months (McKee et al., 1993). SPI advantages are mainly that it relies only on precipitation and its relatively simple computation (Kumar et al., 2016), while the key limitation is relative to the high sensitivity to the quality and time length of data used, and moreover it does not account for the atmospheric water demand. The Standardized Precipitation Evapotranspiration Index (SPEI) (Vicente-Serrano et al., 2010) and the Palmer Drought Severity Index (PDSI) (Sheffield et al., 2012) overcome this limitation by considering the evapotranspiration besides precipitation, in order to account for the role of evaporative demand on drought severity.

An alternative approach is to monitor soil moisture (SM) changes over large areas using satellite-based SM products (Sadri et al., 2018), based on microwave sampling techniques with active (Sentinel-1, ASCAT) or passive (SMOS, SMAP, AMSR-E) technologies (Kerr et al., 2010; Bauer-Marschallinger et al., 2018). However, inconsistencies among the different products have been documented with correlations ranging from 0.48 to 0.89 among them and ground data (Cui et al., 2017; El Hajj et al., 2018; Paciolla et al., 2020). This might be mainly due to different sensing techniques, spatial resolutions (from 50 km of SMOS to 1 km of Sentinel1), the sensing soil depth of few centimetres, which is not congruent with the hydrological active soil for plant root zone uptake. Moreover, there are problems linked to the saturation of soil moisture retrieval algorithms for active radars (Giacomelli, et al., 1995) and their ability to detect soil moisture over vegetated surfaces (Bindlish and Barros, 2001). Notwithstanding these issues, remotely sensed soil moisture products are widely diffused in the scientific community, thanks to the possibility of overcoming the great limitations of retrieving soil moisture through ground measurements, from costs to representativeness of point-wise measurements over a largely heterogeneous areas (Famiglietti et al., 2008; Crow et al., 2012). An extensive review of numerous applications of remote sensing SM, despite their possible uncertainties, is provided by Babaeian et al. (2019).

A less common approach for drought monitoring involves the use of a Land Surface Temperature (LST) derived index (Kogan, 1997; Sepulcre-Canto et al., 2012), computed using the thermal infrared (TIR) spectra on-board a few numbers of sensors (MODIS, LANDSAT, Sentinel-3) (Jiménez-Donaire et al., 2020). On the other hand, the LST is widely used in energy or energy-water balance models to compute evapotranspiration (Kustas and Norman, 1999; Su, 2002; Corbari and Mancini, 2022), while for longer periods analysis is almost unused mainly due to data unavailability during cloud conditions and the non-unique relationship between LST and SM (Price, 1980).

Several satellite vegetation indices might be used to monitor the effect of droughts directly on vegetation, as the NDVI index, which however might be limited in its use by other external factors (e.g. soil adjacency), or the normalized difference water index (NDWI) which accounts for the water leaf contents, or the fraction of absorbed photosynthetically active radiation (fAPAR) (Choudhury, 1987).

Moreover, these anomalies are sometimes asynchronous with respect to each other, as for example soil moisture and vegetation ones (van Hateren et al., 2021), due to the delayed response of vegetation to water scarcity. Another discrepancy could be related to vegetation anomalies not associated to water availability, which can lead to issues in defining agricultural droughts and hence false drought identifications. To overcome this inconsistency, it is thus important to detect the different droughts on SM and vegetation.

Thus, for operative applications for supporting policymakers, water managers and stakeholders, a combination of indices is an optimal solution to detect the different droughts and their impacts, allowing to account for the specificities of different climatic-anthropogenic regions (Hoffmann et al., 2020). In the last few years, some operational drought monitoring and early warning systems have been developed at continental scales, by assembling a suite of independent indices which detect the different type of droughts, to be able to provide water shortage trends and deviations from the long-term averages of mainly precipitation, streamflow, soil moisture and groundwater (Sheffield, et al., 2014; Vogt et al., 2018). Among them, the United States Drought Monitor (https://droughtmonitor.unl.edu), based on different indices at weekly scale, or the Global Integrated Drought Monitoring and Prediction System (GIDMaPS, http://drought.eng.uci.edu, now non-operational), or the Combined Drought Indicator (CDI) (Sepulcre-Canto et al., 2012) revised by Cammalleri et al., (2021) for considering the consistency of prolonged and interrupted drought events, which is used into the European Drought Observatory (EDO, https://edo.jrc.ec.europa.eu) for detecting European droughts. The CDI combines different indices: (SPI, remotely sensing fAPAR and soil moisture from a hydrological model), each based on different temporal scales, allowing to define three drought categories: watch with precipitation below normal, warning when the precipitation deficit is propagated in soil moisture deficit, alert when it also affects the vegetation.

Such complex, multi-dataset drought monitoring systems are already employed in other regions of the planet (Leeper et al., 2022):

Luan et al. (2015) designed a drought monitoring/forecasting approach coupled with an irrigation management system, encouraging its application in northern China; Ozelkan et al. (2016) focused more on the sensing aspect of drought detection, discussing the differences between rainfed and irrigated cropland when using satellites to monitor droughts over a semi-arid agricultural area (south-eastern Anatolia, Turkey); finally, Wu et al. (2015) applied MODIS data over the US corn belt (midwestern US, from Nebraska to Ohio) to select the best index that could capture the local agricultural drought of 2012, identifying the normalized difference infrared index as a powerful and promising tool to monitor drought conditions over irrigated land. The optimal solution to validate these drought monitoring systems, indexes and indicators is to relate their findings to drought impacts.

In this framework, this work is answering to the question if it is possible to develop an EO-based agricultural drought monitoring indicator (ADMIN) for operative irrigation networks management. The monitoring indicator has been developed following the principle of the temporal evolution of the drought process, by firstly considering the meteorological and agricultural droughts, vegetation water stress and drying. Different drought severity levels are then assigned based on the combination of the different droughts' indices, starting from "no drought" up to "extreme drought". This drought monitoring indicator is developed identifying the relationships between the causes (lack of precipitation, high temperatures and radiations) and effects (soil moisture shortage, vegetation water stress and vegetation drying). Such links provide an indicator for water stress and crop failure monitoring for activating crops protection actions, as irrigation. The robustness of the developed ADMIN will be evaluated by assessing the effect of a drought event on irrigation volumes and crop yields at Irrigation Consortium Scale, as water availability is indirectly affected by all the effects of a drought event. The methodology is applied in two Italian cases studies: the Chiese and Capitanata Irrigation Consortia, which are located in the North and South of Italy, respectively. These areas mainly differ for climatic conditions, crops types, strategies and techniques of irrigation. The analyses are performed over 20 years for the period from 2000 to 2019.

The main innovations rely on: i) the analyses of ADMIN which is usable for operative water management from regional to farm scale; ii) the direct comparison of the drought monitoring indicator on the effective used irrigation volumes and the crop yields at Irrigation Consortium Scale over different years to determine its robustness, iii) a method which is fully based on remote sensing data, differing on sensing techniques, spatial and temporal resolutions, to detect the full drought process development; iv) capability of following the temporal evolution of the drought process, considering a specific variable for each process: rainfall anomaly for detecting the meteorological drought, soil moisture anomaly for the agricultural drought, LST anomaly to detect the vegetation water stress and vegetation indices for plant drying.

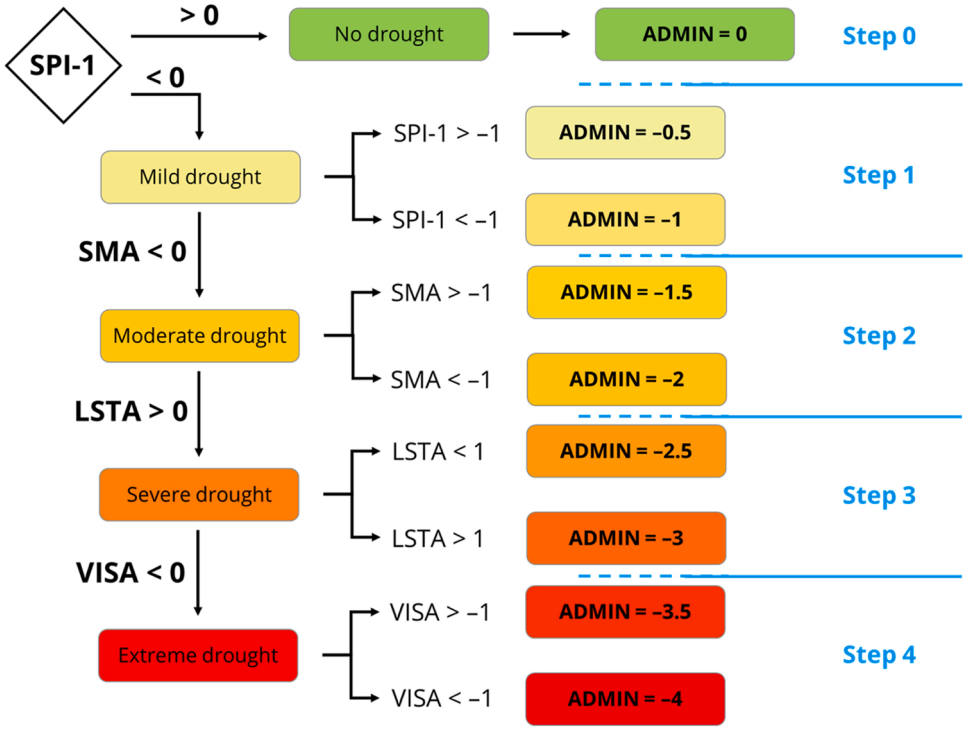

Fig. 1. Possible values of the ADMIN drought indicator according to the anomalies' combinations. SPI-1 identifies the 1-month Standardized Precipitation Index, SMA the Soil Moisture Anomaly, LSTA the Land Surface Temperature Anomaly and VISA the Vegetation Indices Anomaly.

2. Materials and methods

2.1. The agricultural drought monitoring indicator: admin

Following the principle of the temporal evolution of the drought process (Wilhite and Glantz, 1985), the meteorological drought occurs first (a period with less rainfall than average, according to the SPI index), and it generally precedes the agricultural drought, when crop production may be reduced due to soil moisture shortage. This shortage can further increase the drought severity, leading to an increase of crop surface temperature (observed by vegetation water stress indices) and finally to vegetation drying.

Drought-related aspects often have an embedded uncertainty especially related to the definition and detection of drought indicators as well as in the impact assessment and reporting. The fuzzy theory, introduced by Zadeh (1978), could be a way in handling these uncertainties by allocating fuzzy values when objective metrics struggle to adequately measure their magnitude (Huang et al., 2015; Shyrokaya et al., 2024). Thus, the ADMIN indicator is based on fuzzy categories for the drought level. ADMIN is divided into 4 levels, representative of each drought step and assigned considering the anomaly of each variable, starting from no-drought condition, till extreme drought. Each level is further characterized depending on the severity of the event, adopting the −1 threshold identified by Komuscu (1999) and McKee et al. (1995) to distinguish milder (>-1) and stronger (<-1) drought sub-levels. This classification aligns with similar categorizations of drought severity outlined by WMO (2016) or EDO (2020). The four steps are:

1) precipitation deficit is assessed using the standardized precipitation index (SPI-1, 1-month accumulation period) index: if positive values are registered, no drought is recorded (ADMIN takes a null value). On the other hand, if negative values are registered, a mild drought is recorded and depending on the value of SPI-1, ADMIN can take on a milder (-0.5) or stronger (-1) value;
2) soil moisture shortage is evaluated via the soil moisture anomaly (SMA): for negative values, a moderate drought is defined, with ADMIN taking on the values of −1.5 or −2, depending on the magnitude of SMA;
3) vegetation drying is identified with a positive land surface temperature anomaly (LSTA), indicating a severe drought, with ADMIN values of −2.5 or −3 based on the value of LSTA (only for this anomaly indicator, LSTA<+1 is associated with milder conditions and LSTA>+1 with stronger conditions, as higher surface temperatures are associated with harsher drought conditions);
4) vegetation stress is estimated by the vegetation indices anomaly (VISA), labelling the event an extreme drought, which could be represented by ADMIN values of −3.5 or −4, depending on the value of VISA.

During the irrigation season (from April to October) irrigation is added to precipitation. The steps described above for the drought indicator computation are shown graphically in Fig. 1.

All the anomalies employed by ADMIN to evaluate drought conditions are evaluated as the deviation of a given parameter from its long-term mean value (Eq.1). This procedure allows to remove the underlying seasonality signal via the formulation:

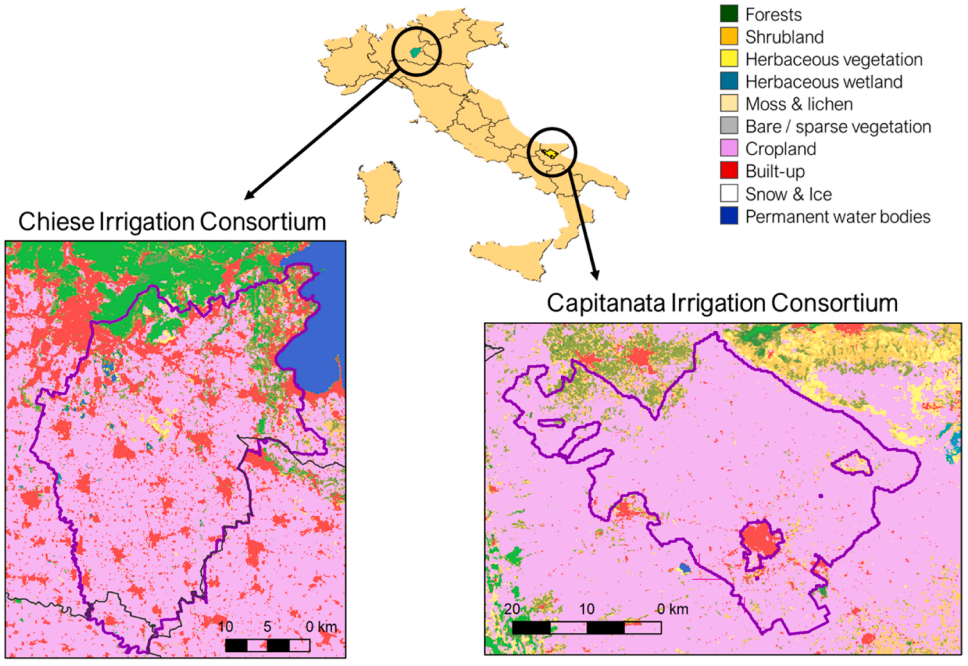

Fig. 2. The location of the Chiese and Capitanata Irrigation Consortia within Italy. The two zooms show the land use/cover maps of the Consortia, highlighting the predominance of cultivated areas (ESA WorldCover 2021 map (https://worldcover2021.esa.int)).

$$Anomaly = \frac{X_{i_d} - \overline{X}_d}{\overline{\sigma}_{X_d}} \quad (1)$$

where X_{i_d} is the variable value at the i-th time step within dataset d, $\overline{X}_d$ and $\overline{\sigma}_{X_d}$ are respectively the mean and standard deviation calculated along the same dataset d. The anomalies are computed at daily scale, updating the variables value whenever the corresponding satellite observations are available for soil moisture and land surface temperature, comparing each value X_{i_d} against the average and standard deviation of the same variable X in the same day of the year i.

The ADMIN indicator is updated daily, so that the time scale evolution is consistent with the water management practices of the two considered case studies. Instead precipitation anomalies are updated monthly in line with the scientific literature (McKee et al., 1993).

The Standardized Precipitation Index (SPI) (McKee et al., 1993) represents the probability that a certain location would receive at least the observed amount of precipitation over a certain time period. Different aggregation times are employed in the literature, from 1 month up to 24 (Shyroaya et al., 2024). In this work, 1-month SPI (SPI-1) was chosen, in order to capture immediate impacts on the crop (e.g., reduced soil moisture availability). Longer time horizons would better identify long-term effects, but in ADMIN these are covered by the anomalies of other remotely-sensed variables, which would have resulted in a redundancy of information. The SPI is computed fitting the gamma probability distribution (Thom, 1958; Abramowitz and Stegun, 1964).

2.2. Case studies and data

The methodology is applied in two cases studies: the Chiese and Capitanata Irrigation Consortia, which are located in the North and South of Italy, respectively (Fig. 2). These two areas are highly cultivated, as from the land cover/use map (Fig. 2) and are representative of the heterogeneity of Italian agriculture (Chiese and Capitanata), as they span different climatic conditions (humid and semi-arid), crops types (water-demanding maize and soybean and fresh vegetables-winter wheat), water availability and source (lakes and groundwater), irrigation techniques (flood and drip) and distribution rules (fixed-scheme and on demand). These differences will help to demonstrate the robustness of the implemented methodology.

Both areas have experienced drought periods in the past, especially the Capitanata one, where due to very high temperatures and water shortages during August 2012, the production of tomatoes was affected with a reduction in yield that exceeded 20–25%. Similarly, during the drought of July 2017, the account of the damages exceeded 2 billion of euro (Coldiretti, 2017).

The Chiese Irrigation Consortium (www.consorziodibonificachiese.it) provides irrigation to an area of about 20'000 ha in the Pianura Padana Plain near the Lake Idro covering the province of Brescia in the North of Italy. The climate is classified as humid subtropical (Cfa) as from the Koppen classification), with winter cold temperatures and hot and humid summers. The annual average precipitation is 700 mm, mainly concentrated in autumn, with more than 200 rainy days a year. The area is intensively cultivated with summer crops as maize and forage, and winter wheat. During summer, crops are sustained by high irrigation volumes provided on a prior fixed turn every 7 ½ days from April to September. Irrigation is mainly provided using the surface technique, and water is withdrawn from a dense channel network diverted from the river Chiese downstream the Lake Idro. An average irrigation volume of about 1200 mm is provided during the crop season (irrigation volumes are planned in advance by the consortium and monitored daily), over a mean precipitation value of 250 mm.

In contrast, the Capitanata Irrigation Consortium (www.consorzio.fg.it) extends for an area of 50'000 ha in the province of Foggia in the Puglia region in the South of Italy. The climate is classified as hot-summer Mediterranean (Csa) as from the Koppen classification), with hot and dry summers. The annual average precipitation is 500 mm, mainly concentrated in autumn and winter, with less than 100 rainy days a year. The area is characterised by intensive agriculture with summer tomatoes (17% of the area), and autumn and winter fresh vegetables (24% of the area), olives and vineyards (34%), and winter-spring wheat. Irrigation is provided on demand

Table 1
Spatial dataset sources and characteristics.

	Dataset	Retrieval technology	Revisit time	Used time period	Product grid	Source
Precipitation	ECMWF ERA5	reanalysis model	hourly	2000–2020	31 km	Hersbach, H. et al., 2018
Soil moisture	SMOS	Passive (L band)	1–2 days	2010–2020	25 km	Kerr, 2010; Al Bitar et al., (2017)
	SMAP	Passive (L band)	2.2 days	2015–2020	36 km	Entekhabi, 2012
	ESA-CCI	Active Passive Combined	1.2 days	2000–2020	25 km	Gruber et al., (2019)
	Copernicus S1 (Sentinel1)	Active (C band)	4.1 days		1 km	Bauer-Maschallinger et al., 2018
	FEST-EWB hydrological model	energy water balance	hourly		30 m	Corbari et al., 2011
LST	Landsat 7–8	Thermal infrared	8/15 days	2000–2020	30 m	Skokovic et al., 2019
	MODIS	Thermal infrared	daily	2000–2020	1 km	Sobrino et al., 2000
Vegetation index (NDVI, NDWI, SAVI, EVI)	Landsat 7–8	VIS NIR	16 days	2000–2020	30 m	Skokovic et al., 2019; Corbari et al., 2020
	MODIS	VIS NIR	8 days	2000–2020	500 m	Myneny et al., 2002

through a metered pressurized network pumping water from two reservoirs, from April to October. The fields are averagely watered with a seasonal amount of 600 mm plus a rainfall mean of about 150 mm, mainly with drip and micro-sprinklers techniques.

2.2.1. Data sources

The considered dataset encompasses different variables (precipitation, soil moisture, land surface temperature and vegetation indices) which could be obtained from different sources (remote sensing, ground data and hydrological land surface model) at different spatial and temporal resolutions (Table1). A benchmark combination of data products for the ADMIN computation is identified in order to maximize the length of the dataset, allowing to have a time series from 2000 to 2020, to be able to produce a robust statistic based on 20 years of data. The benchmark ADMIN was computed considering the ERA5 precipitation data, for soil moisture anomaly the ESA-CCI Combined dataset, for the land surface temperature and the vegetation anomalies the MODIS data were chosen.

2.2.1.1. precipitation. Precipitation data are obtained from the ERA5 database provided by ECMWF (European Centre for Medium-Range Weather Forecasts) (Hersbach et al., 2020). ERA5 is a reanalysis dataset which provides the description of land water and energy cycles over several decades from 1950, combining the high-resolution ECMWF land surface model driven by the downscaled meteorological forcing from the ERA5 climate reanalysis (Hersbach et al., 2020) with observations from across the world into a globally complete and consistent dataset. ERA5 is freely available through the Copernicus Climate Change Service (Hersbach et al., 2018). Beck et al., (2017) showed that this dataset has the best performances among several other reanalysis datasets and satellite data.

2.2.1.2. satellite soil moisture datasets. Satellite retrieval of soil moisture presents numerous perks (Babaeian et al., 2019), but nonetheless displays high variability among the different available products.

The Soil Moisture Ocean Salinity (SMOS) is a European Space Agency (ESA) Earth explorer mission launched in 2009 (Kerr et al., 2010), which provides SSM data at 25 km of spatial resolution twice every day.

The SMOS Root-Zone soil moisture product is provided by Al Bitar et al. (2013). It employs SMOS L3 surface soil moisture and other data (e.g., NDVI from MODIS, climate data from ECMWF) to derive soil moisture at root level using an exponential filter for the first soil layer and a physical model for the second.

The Soil Moisture Active Passive (SMAP) mission from the National Aeronautics and Space Administration (NASA) provides surface soil moisture products at 36 km from L-band microwave data (Entekhabi et al., 2014).

The ESA Climate Change Initiative (CCI) (Gruber et al., 2019) dataset is the final product of a wide effort aimed at standardizing and merging a large range of different SSM datasets gathered throughout the years into one global database. It merges active remote sensing (from AMI-WS, ASCAT-A and ASCAT-B) and passive one (SSMR, SSM/I, TMI, AMSR-E, Windsat, SMOS and AMSR2). Finally, the ESA-CCI Combined dataset is obtained by scaling both databases to a common product (GLDAS Noah) (Dorigo et al., 2017).

The Copernicus Surface Soil Moisture 1 km Version 1 product (SSM1km) is the result of the Sentinel-1 SAR backscatter observation in band C. It provides relatively high 1 km spatial resolution, although its revisit times are slightly longer, around 4 days (Bauer--Marschallinger et al., 2018).

2.2.1.3. satellite land surface temperature. Satellite Land Surface Temperature (LST) has been retrieved from MODIS low resolution data and from the high-resolution LANDSAT series.

The used MODIS LST product (http://ladsweb.nascom.nasa.gov/index.html) is MODIS/Terra LST/E Daily L3 Global 1-km Grid product (MOD11A1) at a spatial resolution of 1 km and a daily temporal resolution (Wan, 2008).

Landsat 7 ETM+ and Landsat 8 satellite data have also been considered (USGS, http://earthexplorer.usgs.gov/), with LST data provided at a spatial resolution of 30 m and a temporal frequency of 16 days. Land surface temperature is computed using the Single Channel surface temperature retrieval algorithm, based on the Radiative Transfer Equation which can be written in the thermal infrared region as Jimenez-Munoz et al. (2014).

2.2.1.4. satellite vegetation indices. Different vegetation indices (VIs) might be retrieved from remote sensing data to describe the evolution of an agricultural drought, taking advantage of their characteristics of detecting vegetation changes. It is still an open problem in literature which index best represents the crops stress and dynamics (Huete et al., 1997).

Among them, the Normalized Difference Vegetation Index (NDVI) is the most widely used, representing an indication of plants greenness and their photosynthetic activity, responding to changes in the chlorophyll content and the intracellular spaces in spongy mesophyll of plant leaves. NDVI is computed as the normalized difference between the near infrared (NIR) and visible red reflectance.

Additionally, the Soil Adjusted Vegetation Index (SAVI) was also considered as an index able to reduce the soil background effect (Huete, 1988); or the Normalized Difference Water Index (NDWI) (Gao, 1996) which allows estimating the vegetation water content based on shortwave infrared band reflectance increases or decreases. It is sensitive to variations in the water content (absorption of SWIR radiation) and spongy mesophyll (reflectance of NIR radiation).

Finally, the enhanced vegetation index (EVI) is also considered, in order to detect the minimization of the canopy-soil variations and its sensitivity over dense vegetation.

The Moderate Resolution Imaging Spectroradiometer (MODIS) data used in this study (Table1) are the 8-day composite (the best quality daily reflectance data of the 8-day period), 500-meter dataset MOD13A1. The products of NDVI, NDWI, EVI and SAVI are directly used. As the vegetation indices are an average of 8 days, the index value is kept constant for the time period of 8 days. At high spatial resolution, the vegetation indices are computed from Landsat 7 and 8 satellite images at 30 m spatial resolution.

2.2.2. Crops yield data

Crops yield estimates are available from the Italian National Statistics Institute (ISTAT, https://www.istat.it/it/agricoltura?dati). Total yield and total cultivated areas for the main cultivated crops are provided by Province. For the Capitanata area, the province of Foggia is selected, as most of its agricultural activity is found within the Capitanata Consortium (95% of its area, or 47'000 ha). The Province of Brescia is chosen, as it covers almost all of the Chiese Consortium Area.

3. Anomalies analysis

The anomalies of precipitation, soil moisture, land surface temperature and vegetation computed over the Capitanata and Chiese Consortia for the years from 2000 to 2020 are reported in Fig. 3 and in Fig. 4, respectively. The chosen combination of data products for the ADMIN computation is identified in order to maximize the time duration length. Besides the ERA5 precipitation data, for soil moisture anomaly the ESA-CCI Combined dataset is selected, for the land surface temperature and the vegetation anomalies the MODIS data are chosen.

Precipitation SPI-1 calculated from the ERA5 reanalysis dataset show marked periods of drought interspersed with periods of higher than average rainfall all along the years, without specific differences during the crop season. The Capitanata area is in general more subject to spring drought conditions for below than normal rainfall than the Chiese area. Important winter droughts are also visible in the last years.

It is important to note that the SPI1 index is the result of a statistical process where precipitation is fitted with a gamma distribution on non-zero values per month of the year and then normalized. For dry climates, where zero precipitation values are common, such as the case of South Italy, the calculation of SPI might be skewed (Wu et al., 2007). Therefore, the application of SPI is critical and its interpretation must be done properly.

Soil moisture anomalies are calculated for each available date based on monthly variations at daily scale considering the ESA CCI Combined dataset, as the most complete series from 2000 to 2019 for both case studies. A strong signal is found with negative SMA in summer and positive SMA values in winter. SMA is also characterized by some severe drought conditions, as the spring-summer months of the years 2007–2008 and 2016 in the southern area, or the summer periods of the years 2003 and 2019 or the winter of 2011–2012 in the northern area.

LST series retrieved from MODIS at 1 km of spatial resolution are averaged over the analyzed area and used to calculate LST anomaly. Positive values of LSTA represent warmer days, where the LST is higher than the mean value and water stress is liable to occur, whereas negative values identify the colder-than-average days. For the Capitanata Consortium, a higher number of highly-negative anomalies are detectable during the summer season. This might be due to the fact that only the 40% of the area is cultivated during summer with highly irrigated crops (mainly tomatoes) while the remaining part is cultivated with winter rainfed wheat or bare soil (Corbari and Mancini, 2022).

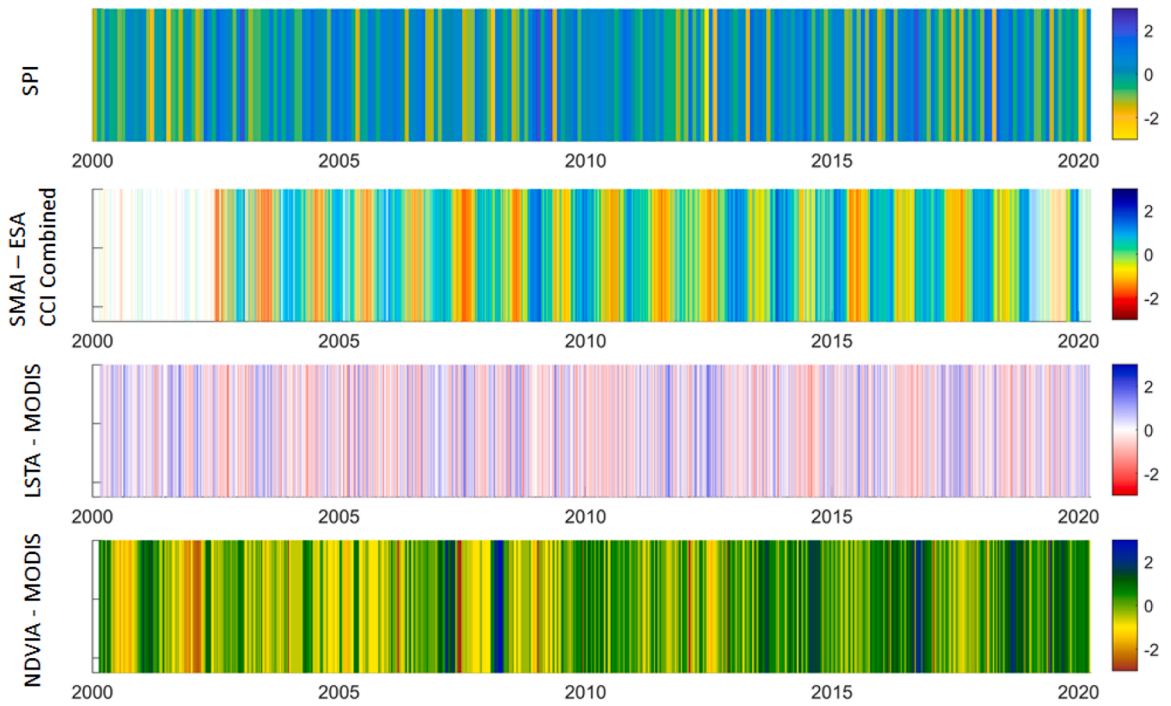

Fig. 3. SPI-1 monthly index based on the ERA-5 dataset, SMA daily soil moisture anomaly from the ESA-CCI Combined dataset, daily LSTA anomalies from MODIS and daily NDVI anomalies from MODIS for the Capitanata Consortium from 2000 to 2020.

Fig. 4. SPI-1 monthly index based on the ERA-5 dataset, SMA daily soil moisture anomaly from the ESA-CCI Combined dataset, daily LSTA anomalies from MODIS and daily NDVI anomalies from MODIS for the Chiese Consortium from 2000 to 2020.

It is worth to remember that a monthly anomaly is computed, so that the trend seasonality is removed with no default low values in autumn/winter and high values in spring/summer.

Similar results are obtained for the Chiese area with no specific seasonal stress periods. However contrary to Capitanata, the summer period is usually characterized by several days of high positive anomalies. This due to the fact that the Chiese area is mainly cultivated with irrigated corn.

Vegetation indices anomalies are finally considered to detect and monitor the impacts on vegetation growth and productivity of environmental stress factors, especially plant water stress due to drought. As NDVI from MODIS is provided as an average over 8 days, to compute the daily VISA anomaly, the same NDVI value is kept constant for 8 days. VISA shows for the Capitanata area strong negative values during the summer months for the years 2000 and 2001, as well as for the years 2007 and 2008. These findings are consistent with the evolution of the drought, which showed also strong negative SMA values. On the contrary, for the Chiese area no highly negative anomalies on vegetation are observed, except for the summer of 2003 where to negative VISA corresponds also negative SMA values. Instead to the negative SMA of the 2019 summer, a positive VISA is obtained.

It should also be noted that vegetation indices could also catch senescence periods shifted in the different years according to the year specific climate; such negative anomalies would not then represent drought conditions. However, as VISA is considered within ADMIN only in the very last step, after considering the anomalies of the other variables, the impact of these misrepresented senescence periods on the ADMIN index is expect to be negligible.

3.1. Synchronism and correlations among anomalies

The synchronism (or its absence) among the different variables' anomalies is further analyzed during the different years to understand how a precipitation drought could lead to a soil moisture one, which in turn might or not be transferred to temperature and vegetation droughts. The temporal consistency between a pair of variables is defined building a contingency table: a positive agreement is recorded when both variables report either drought or absence of it, whereas a disagreement is assigned when one variable reports drought conditions, and the other does not. The differentiation between the two conditions is based on the sign of the anomaly, with drought conditions associated with negative anomalies (except for LST). Then, the percentage of days of the four possible combinations of the contingency tables are computed. Three possible combinations of variables' anomalies are shown averaged over each month in Fig. 5 for the Capitanata and Chiese Consortia areas, highlighting differences between the two.

In the Capitanata Consortium, considering SPI and SMA, a consistency of 40% is found with both negative anomalies during the summer months, and of 50% for only a negative SM anomaly for the same period. This is in line with the characteristics of this agricultural area, which is generally very dry in summer with few precipitation events and only 40% of the area is cultivated with irrigated crops. During the other months of the year, the conditions of no drought or of opposite signs of the anomalies (mainly due to a negative SPI anomaly) prevail. Hence, the Pearson correlation coefficient over the whole period between SPI and SMA is quite low

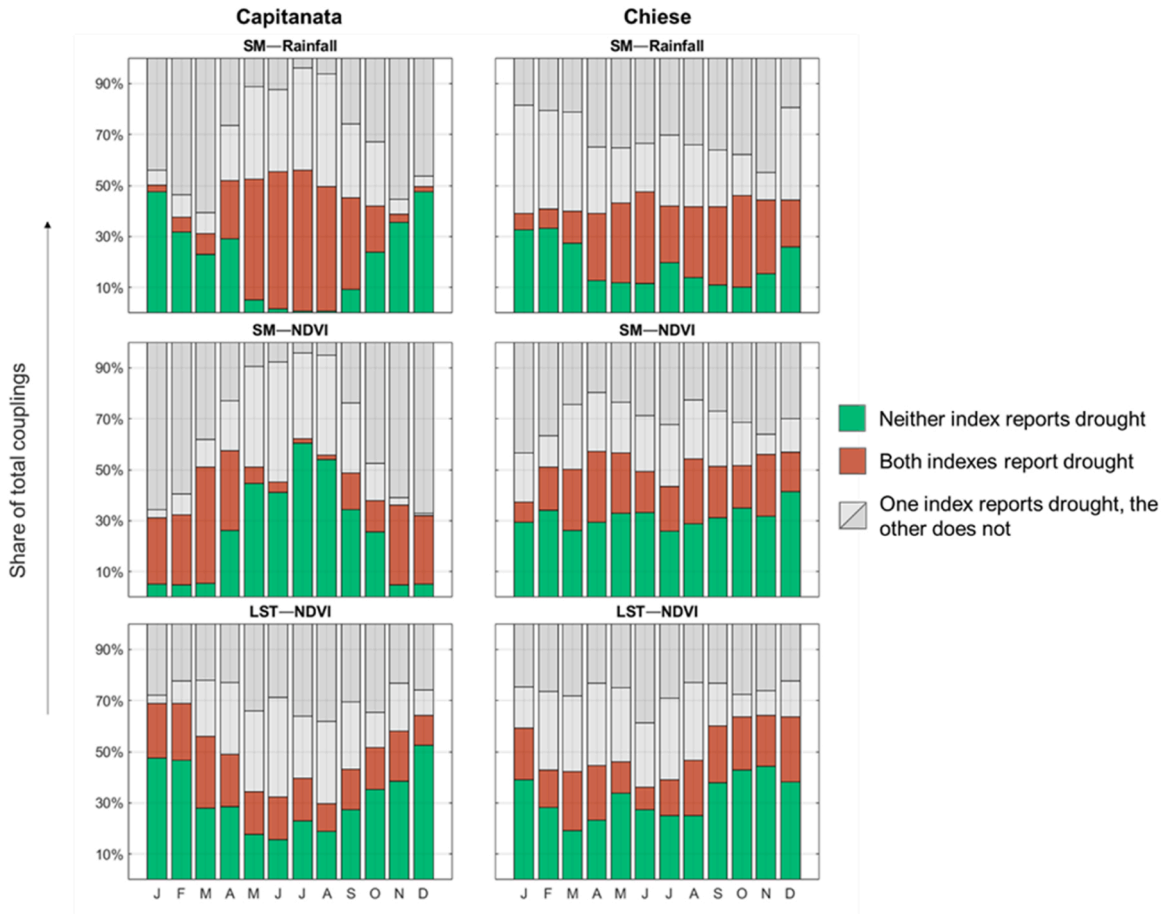

Fig. 5. Synchronicity among anomalies of soil moisture, precipitation, NDVI and LST in the Capitanata (left-hand column) and Chiese (right-hand column) Consortia from 2000 to 2020.

(0.2). SMA and VISA agree on drought conditions roughly 40% of the time. This situation might be due to the fact that the vegetated areas are mainly irrigated and the NDVI index obtained from the MODIS dataset at 1 km of spatial resolution is able to catch these differences, while the soil moisture from the low spatial resolution dataset (25 km) is not detecting the differences between irrigated and not irrigated fields, but only the average area value. Moreover, it might be related to the different time response of the index to drought (e.g. precipitation is the first while vegetation is the last). In general, a low and positive Pearson coefficient (0.23) is found between SMA and NDVIA all over the years.

A high seasonal dynamic of anomalies consistencies is also registered between SMA and LSTA (not shown), with a consistency of 50% indicating both drought conditions as well as only SM stress during the summer months. This is in line with the obtained results between SMA and VISA, as well as similar explanations could be given on the response of LST to SM conditions. A negative Pearson correlation is found (-0.19).

A non-defined trend in the consistencies is instead obtained between SPI and VISA (not shown) as well as between LSTA and VISA (bottom row of Fig. 5), with a non-predominant situation along the year. A positive correlation is obtained between SPI and NDVAI (0.18), while a weak negative one between LSTA and VISA (-0.05). However, LSTA and VISA are negatively correlated only during summer (-0.2), while a positive value is obtained if only winter months are considered (0.33). This might be due to the fact that vegetation stress response delays with respect to water deficit and high temperature.

For the Chiese Consortium (right-hand panels of Fig. 5), a non-seasonal distribution of the consistencies is observable for all variables couples' comparisons, with no predominance of a drought or no drought conditions in any month of the year. The Chiese area is intensively cultivated with forages all the year as well as irrigated, leading to controlled conditions for LST, SM and NDVI.

If SPI and SMA are compared, the Pearson correlation coefficient over the whole period is positive (0.32) with a lower correlation during summer (0.1). This might be simply explained by the fact that in the Chiese Consortium during the summer season when maize crop is largely cultivated (90% of the area), high amounts of irrigation are used, leading to positive SMA anomalies which, however, might be present with negative SPI values.

Conversely to the Capitanata Consortium, the Pearson correlation between SMA and VISA is slightly negative (-0.07), with SM negative anomalies which are usually not reflected into vegetation stress.

As there seems to be no prevailing trend in consistency, all the other variables correlations are very low, being negative the ones between SPI and LSTA (-0.01), SPI and VISA (-0.04) as well as SMA and LSTA −0.01, while a slight positive correlation is obtained between LSTA and VISA (0.1).

4. Agricultural drought monitoring indicator (ADMIN)

As a step forward from the single anomalies, the ADMIN is computed at daily time scale combining the different anomalies (SPI-1 from ERA5, SM from ESA CCI Combined, LST and NDVI from MODIS) with the procedure defined in Fig. 1.

To easily compare how the level of dryness changes in time, the cumulative drought index curve is evaluated for each year, summing all the daily contributions. In Fig. 6, the comparison is reported for both case studies in terms of daily and yearly cumulated values. All the curves have a common behaviour: from the begin of the year till March the curves have gentle slopes, then from March to October they are very steep due to drought conditions, and at the end of the year they return flat. This behavior agrees with the crop seasonality and with the irrigation period. In general, a good accordance is visible among the different series, being the high-resolution series able to accurately reproduce the low-resolution behavior, even if for a shorter time period of analysis. In Capitanata area, the driest years are identified as 2003, 2011, 2012 and 2017, while the wettest years are 2010 and 2014 (Fig. 6). Similarly for the Chiese Consortium, 2010 and 2014 are identified as very wet years, while very dry years are 2003, 2007, 2017 and 2019.

An example of the advantages and strengths of the ADMIN methodology is shown in Fig. 7, for the specific drought event involving the 2012 Capitanata agricultural season. The daily ADMIN values for that year (Fig. 7a) are contrasted with the corresponding single anomalies (SPI-1, SMA, LSTA, VISA, Fig. 7b). The effect of the May-June SPI negative anomaly on the other variables is delayed by at least one month, with VISA still showing low values in July. In general, the precipitation dynamics have high amplitudes, whereas the time periods of the responses from the soil moisture levels and plant wellbeing are quite long, confirming the possible asynchronous behavior of the different variables. On the other hand, the ADMIN catches up the low SPI values and starts to register the effect on vegetation by early June. When SPI reaches close-to-zero values (July), ADMIN levels remain between −2 and −3, due to the negative vegetation anomaly which is still not recovered.

The asynchronies among indices are also visible for the Chiese area for the example year 2003 (Fig. 7). The daily ADMIN starts to decrease at the beginning of the year 2023 with the strong negative increase of all indices (SPI, SMA and VISA), besides LSTA which is increasing. The effect of the reduction of the May-July SPI and SMA negative anomalies on VISA is delayed by at least two months, due to the strong positive anomaly of LSTA.

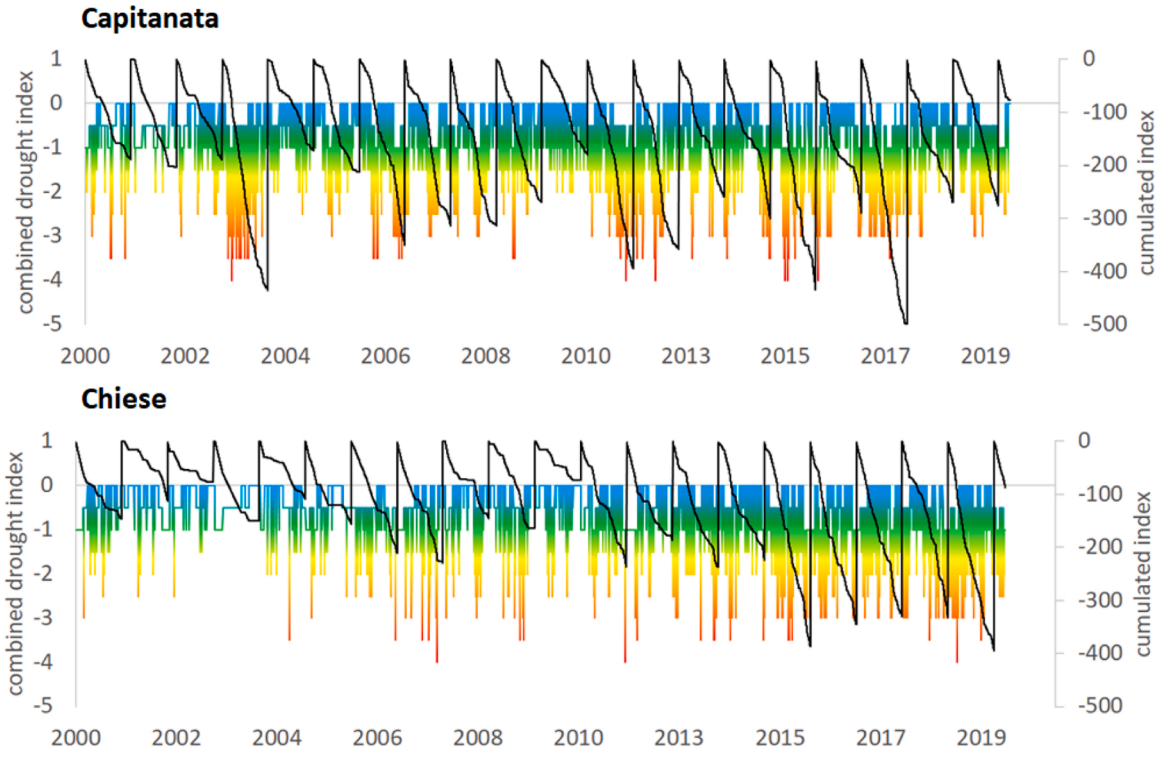

Fig. 6. ADMIN daily values and cumulative yearly values for Capitanata and Chiese Consortia: SPI from ERA5, SM ESA-CCI Combined, LST and NDVI from MODIS.

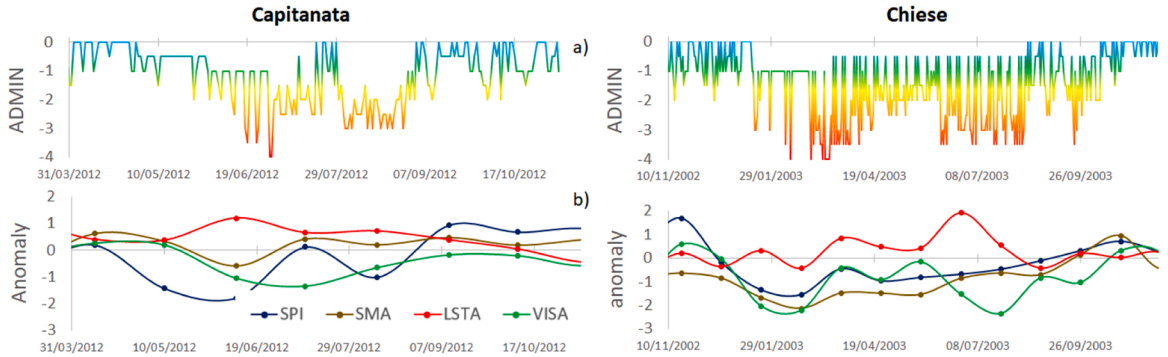

Fig. 7. Example of the application of ADMIN to the agricultural seasons of 2012 for the Capitanata Consortium (left) and of 2003 for the Chiese Consortium: monthly variable anomalies (a) and corresponding daily ADMIN values (b).

4.1. *ADMIN performances*

We can conduct a first qualitative examination of the temporal evolution of the ADMIN combined indicator for each analysed year, by comparing with reference datasets, during the crops growing seasons.

In the Capitanata area, the ADMIN identifies as driest years as 2003, 2011, 2012 and 2017, while the wettest years are 2010 and 2014. A first confirmation of the capability of ADMIN to detect agricultural drought conditions is the comparison with local analyses by the Italian farmers association Coldiretti (https://www.coldiretti.it/), which reports very high temperatures and water shortages during the summer 2003, August 2012 and July 2017, and reduction in tomatoes productions that exceeds 20–25%. Similarly, the Italian government natural calamity report (https://www.politicheagricole.it) confirmed the significance of the 2012 and 2017 droughts, enabling an economic compensation for verified losses surpassing 30% of the production (Ministerial Decree April 18, 2008).

Furthermore, a comparison of drought indications is performed against the European Drought Observatory (EDO, https://edo.jrc.ec.europa.eu), as being the operative reference at European Commission level. An agreement is found between the two drought indicators in the Capitanata area in identifying the driest year for 2012 and 2017, while the EDO is not reporting a vegetation drought in 2012 and no soil moisture drought in 2003. This last year however was one of the driest years in Italy and Europe (Diodato and Bellocchi, 2008; Musolino et al., 2018). Similarly for the Chiese Consortium, 2010 and 2014 are identified as very wet years, while very dry years are 2003, 2007, 2017 and 2019. ADMIN is in general agreement with EDO estimates, except for the year 2017 where no vegetation drought is detected by EDO and for the year 2010 where EDO is not reporting soil moisture positive anomalies. It should be noted that the EDO system is using the FPAR index for vegetation instead of NDVI, and the soil moisture estimates come from a land surface model (Sepulcre-Canto et al., 2012) and not from satellite measurements.

Additionally, the European drought impact report inventory, EDII (Blauhut et al., 2022), is considered, as it lists the impacts of droughts at regional level between 2003 and 2019. Specifically, for the Lombardia region the years 2003, 2012, 2015 and 2017 are identified in EDII as drought years with many reported negative impacts. The ADMIN indicator agrees in identifying those years as the worse drought events. For the Puglia region, the main droughts with reported impacts are identified in the EDII as the years 2008, 2012, 2015 and 2017. The ADMIN indicator is able to detect the relevancy of the drought conditions, especially the important drought events of 2012, 2015 and 2017.

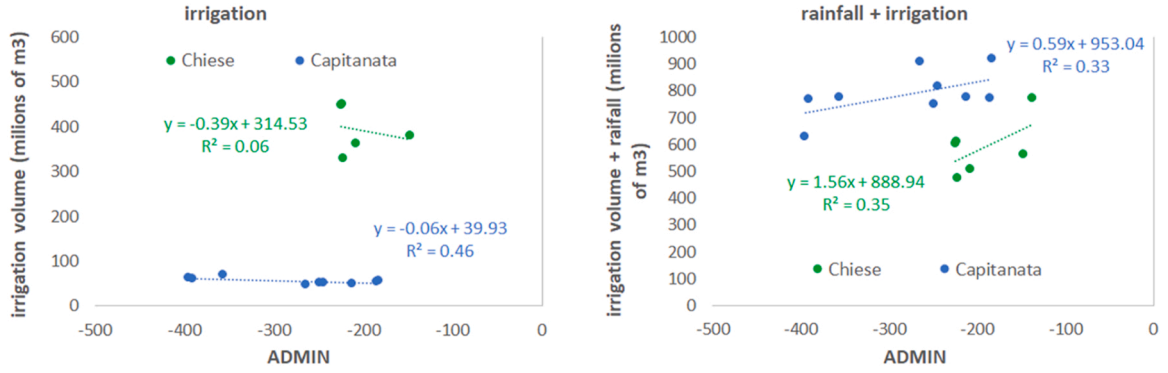

Fig. 8. Seasonal cumulated ADMIN index relationship with irrigation volumes and with rainfall plus irrigation for the Capitanata and the Chiese Consortia.

4.2. Relationship between ADMIN and irrigation volume and crop yield

Irrigation volumes are a way to provide a reliable assessment of the drought impacts and consequently the ability of ADMIN as an index, as one can expect a higher volume of water used for irrigation during stressed conditions.

In the Capitanata Consortium, observed daily cumulated irrigation volumes are provided by the aqueduct from 2006 to 2016, except for 2008 and 2009, from the 1st of April to 31st December for each year. These values are compared to the daily cumulated ADMIN in the same periods of irrigation volumes availability. A difference of about 20'000'000 m^3 of irrigation water volume is found in observed data between the most irrigated year, i.e. 2012 and the least irrigated one, i.e. 2009. By comparing the behaviour of ADMIN and irrigation volumes, it is immediately visible the high consistency among the years, with the driest years (2012 and 2011), characterized by the lowest ADMIN values, being the years with the highest water volumes used for irrigation (not shown). This is confirmed from the scatterplot of the cumulative drought index values and irrigation volume at the end of each year (Fig. 8). A negative relationship is shown, where an increase in the drought index means an increase of dryness conditions, meaning that more irrigation is required.

Furthermore, the ADMIN is also compared to the cumulated volumes of the total water supplied to the fields, by summing the precipitation volume to the irrigation one. A slightly positive relationship is obtained, meaning that during all years, the total amount of water (irrigation + precipitation) provided to crops is similar. This might be explained by the fact that in the Capitanata Irrigation Consortium the farmers pay a quota for m^3 of water used per ha; so that during wetter years, lower irrigation volumes are provided.

An opposite situation is observed in the Chiese Irrigation Consortium (Fig. 8) where the cumulated ADMIN and the irrigation volumes provided by the channels network at the end of each year are compared in a scatterplot. Almost zero correlation is found, with an almost constant amount of irrigation volumes which is provided to the crops every year independently from the drought or not condition. Consequently, if rainfall volumes are added to the irrigation ones, a positive correlation is obtained. This is immediately explainable by the water costs in the Chiese Consortium, where the farmers pay a fixed quota every year per ha independently from the volumes of water used. Hence, during the rainy years, too much water is probably provided to the crops.

As a further validation of the implemented index as well as to understand the impact that possible drought conditions might have on crops production, a crop specific relationship is analysed in the two case studies by comparing the Consortium crop yields and the ADMIN values (Fig. 9).

In the Capitanata Consortium, the crop yield seems to be almost uncorrelated with the ADMIN index. This might be due to the fact that the area is highly irrigated during summer and that the amount of irrigation is capable of contrasting the drought conditions allowing to maintain an almost constant production over the years. The oscillations in contrast might be related to other factors, as changes in pest and diseases. A common problem in the tomato production in the area is the *Phytophthora infestans*, which is especially affecting the crops during conditions of water stagnation. Even if the agricultural drought monitoring index reaches high negative values, these are persistent for few days, which are not enough for affecting the crop production. Moreover, opposite climate extremes as frost conditions or hailstorms during the spring, might also strongly affect crop production, but are not detected by the implemented drought index.

In the Chiese Consortium, a similar null relationship is obtained between the summer irrigated crops yield and the ADMIN index. As well, this area is highly irrigated with an excess of water used, which is not affecting the production. This might be instead affected by other external factors (e.g. hailstorms, pest and diseases).

The relationship is thus having a spread preventing from the conclusion of a direct link with crop production in the analysed case studies.

To further understand the strength of the developed ADMIN indicator, the single anomalies on which it is based, are directly related with the drought impacts. In Fig. 10, three plots, conceptually similar to those in Figs. 8 and 9, are shown, featuring the average value of the single anomalies over the crops season instead of the seasonal cumulated ADMIN, over the Capitanata test case. The strength of

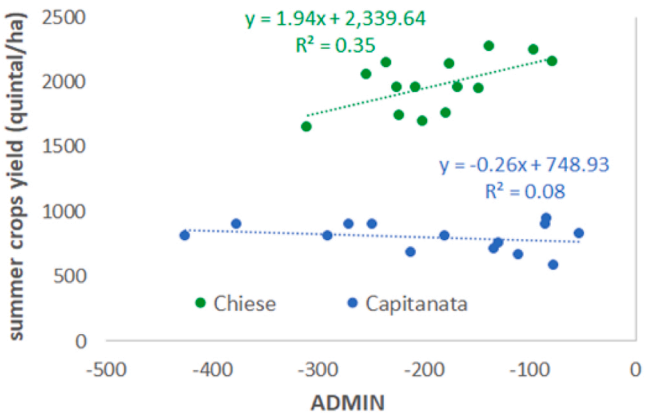

Fig. 9. Seasonal cumulated ADMIN index and crop production relationship, for tomatoes in the Capitanata Consortium and for summer crops in the Chiese Consortium.

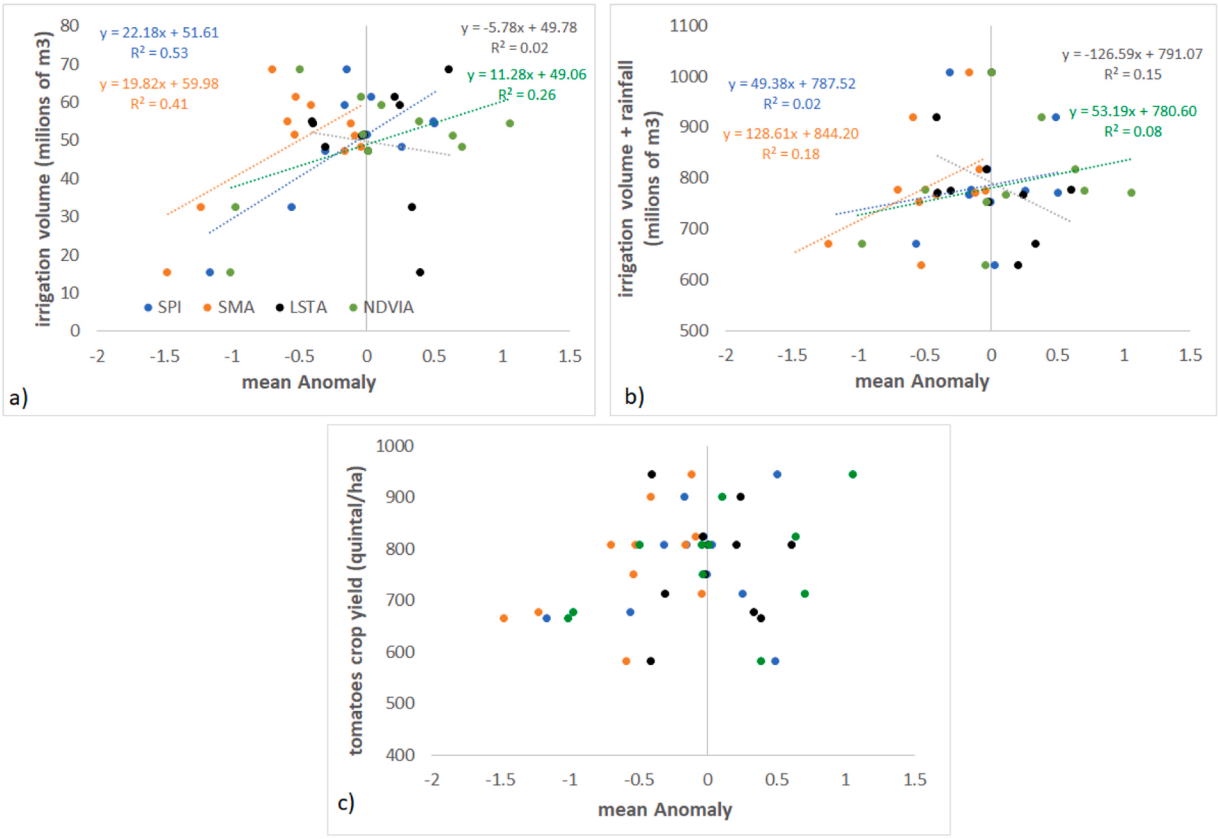

Fig. 10. Relationship between the average value of the single anomalies over the crops season (SPI, SMA, LSTA, VISA) and a) the seasonal cumulated irrigation volume, b) the total seasonal water volume applied to the fields, c) crop production for tomatoes in the Capitanata Consortium.

ADMIN is particularly relevant when the single anomalies are compared with the cumulated irrigation volume, where a positive dependency is found (at higher SPI values lower irrigation water volumes would be expected). Also, a positive relationship is found between SMA and the irrigation events. Moreover, comparing the determination coefficients (R^2) with those from Fig. 8, the relationship between accumulated volume from the aqueduct and single anomaly is everywhere weaker with respect to the ADMIN. This difference is even wider when considering all water inputs (aqueduct and natural rainfall), with the coefficients of determination falling below 0.20. Finally, when looking at the final yield (Fig. 10c), to be contrasted with Fig. 9, a similar behaviour is observed if considering the ADMIN or single anomalies, as the drought effect on the final crop yield is dampened by the irrigation events. Similar conclusions can be drawn for the Chiese Consortium case study.

4.3. ADMIN uncertainties

As many remotely-sensed based products of soil moisture, vegetation indices and land surface temperature are available (Table1), their impact on the ADMIN calculation is evaluated by computing their respective anomalies. The analyses are done according to the

Table 2
Pearson correlations among SMA from different datasets for Capitanata (upper half table) and Chiese (lower half table). The correlations are computed according to the years for which every pair of data is available.

Capitanata / Chiese	ESA CCI- Combined	ESA CCI-active	ESA CCI-passive	SMOS	SMOS-rootzone	SMAP	Copernicus S1	FEST-EWB
ESA CCI- Combined		0.65	-	0.37	0.17	0.34	0.31	0.2
ESA CCI-active	0.79		-	0.41	0.16	0.37	0.41	0.22
ESA CCI-passive	0.78	0.38		-	-	-	-	-
SMOS	0.53	0.51	0.43		0.37	0.41	0.52	0.16
SMOS-rootzone	0.26	0.26	0.12	0.51		0.26	0.22	0.3
SMAP	0.46	0.42	0.48	0.84	0.32		0.47	0.3
Copernicus S1	0.51	0.55	0.39	0.64	0.23	0.55		0.15
FEST-EWB	0.47	0.53	0.38	0.65	0.31	0.47	0.34	

years for which each product is available (Table1).

Firstly, the Pearson correlation coefficient is computed among the different SM datasets anomalies, for both case studies (Table2). This is computed taking each product at a time as reference. Considering the differences in spatial resolution (25 km for ESA CCI, 40/50 km for SMAP and SMOS, 1 km for Sentinel 1–30 m of FEST-EWB), in satellite reading frequency and retrieval algorithm, generally low r values are found with a better correlation in the Chiese area (Table2) (Paciolla et al., 2021). One main distinction between the two test cases is the wetness level: the Chiese case study sees higher average yearly rainfalls (>750 mm/yr, with more than 200 rainy days a year) with respect to Capitanata (550 mm/yr, with 150 rainy days a year). This seems to reflect positively on the correlation between the different SMAs, probably because it corresponds with a more stable, less peaked SM trend, easier to reproduce from products working at different resolutions and with different algorithms. In contrast, the high heterogeneity of the Capitanata Consortium (e.g. high contrast between hot dry bare soil pixels and vegetated wet pixels during summer) leads to lower average correlations among products anomalies.

The results show how the ESA CCI datasets are the ones best correlated to each other overall, even if this result is mainly driven by the fact the ESA CCI Combined dataset includes the other two (Active and Passive). Similarly, the data from SMOS, SMAP and S1 are weakly correlated to ESA CCI data and among each other, showing that no further contribution seems to be provided by higher-resolution information. The data of the FEST-EWB model are similarly correlated to all the others, with a uniform distribution over the two case studies. In particular, soil depth representativeness of the remotely sensed products is 7–10 cm while it is of 60 cm for FEST-EWB. Also, the length of the different datasets doesn't seem to impact on the results, being the SMOS one available from 2000 while Sentinel 1 and SMPA only from 2014 and 2015, respectively.

The adequacy between the LST anomaly calculated from MODIS and Landsat data is also calculated, with a RMSE equal to 0.1 °C and a Pearson coefficient of 0.73. These results agree with the validation of LST estimates (i.e., not anomalies) as obtained by Jimenez-Munoz, et al. (2014), or Corbari et al. (2020) who compared LANDSAT 7 and 8 against ground data with mean absolute differences close to zero with an RMSE of 3.0 K and of 2.0 K for LANDSAT 7 and 8, respectively. As well, Duan et al. (2019) obtained for MODIS daytime data RMSE values around 2 K.

A similar analysis has been performed for the vegetation indices anomalies, as it is still an open problem in literature which index best represents the crops stress and dynamics (Huete et al., 1997). Hence, anomalies are calculated for all the vegetation indices NDVI, NDWI, EVI and SAVI from MODIS and compared. The inter-comparison between the indexes is shown by the Pearson correlation coefficients in Table3. In general, the best alignment is observed between NDVI and SAVI, with negative/positivize anomalies detected in the same periods; the similarities between NDVI and EVI are somewhat weaker; finally, some inconsistencies are detected between NDVI and NDWI, with some peaks with opposite signs. As it is well known, NDVI is strongly correlated to leaf area color and low values are synonymous of vegetation stress with a reduced photosynthetic capacity, while NDWI is linked with the crops leaves' moisture. The opposite peaks are caused by precipitation events that produce an immediate increase in the NDWI values but not in the NDVI, that is always affected by a delay in the response. However, Gu et al., (2008) found that both indices might be suitable for vegetation drought analysis.

Moreover, while NDVI estimates might be influenced by soil background conditions and non-drought stress conditions, such as plant disease (Xue and Su, 2017), similar anomalies changes are detected with SAVI index, which on the contrary is not influenced by soil effects (changes in soil color or soil moisture). The EVI index which accounts for the interaction of the atmospheric conditions (Liu and Huete, 1995), is similarly correlated to NDVI and SAVI anomalies.

The impact of using the different soil moisture products in ADMIN is further evaluated for both case studies, keeping fixed the products for the anomaly calculation of precipitation, vegetation and temperature in respect to the ADMIN computed with the benchmark configuration (as defined in Section 2.2.1 Data sources: ERA5 for precipitation, ESA-CCI Combined dataset for SMA, MODIS data for both LSTA and the vegetation anomaly) while changing one at a time the soil moisture product. The relative yearly difference is thus computed and reported in the color scale of Fig. 11. The ESA CCI Active and Passive products provide generally lower yearly ADMIN values, indicating harsher drought conditions. This happens especially in the early 2000 s, specifically for the Active product across both case studies. The ESA CCI Passive product, not available for the Capitanata case study, in the Chiese area shows a higher divergence from the ESA CCI Combined one. The case of SMOS is of interest, as both the superficial and root-zone products are available: over both areas, the superficial product leads to lower values of yearly ADMIN (harsher drought), whereas the root-zone one is generally more in agreement with the ESA CCI Combined-powered ADMIN, apart from some higher values (milder drought) around the early 2010 s. Finally, the SMAP product (available for only 5 years) generally indicates drier conditions. One possible explanation for the differences could be that the "hybrid" nature (joining both Passive and Active datasets) of the ESA CCI Combined product makes it hardly comparable with more "exclusive" products (either Passive or Active). The hybrid nature of SMAP would call for more

Table 3
Pearson correlations among different vegetation indices anomalies for Capitanata (upper half table) and Chiese (lower half table). The correlations are computed according to the years for which every pair of data is available.

Capitanata / Chiese	NDVI	EVI	SAVI	NDWI
NDVI		0.65	1.00	0.49
EVI	0.5		0.65	0.35
SAVI	1	0.5		0.49
NDWI	0.44	0.44	0.44	

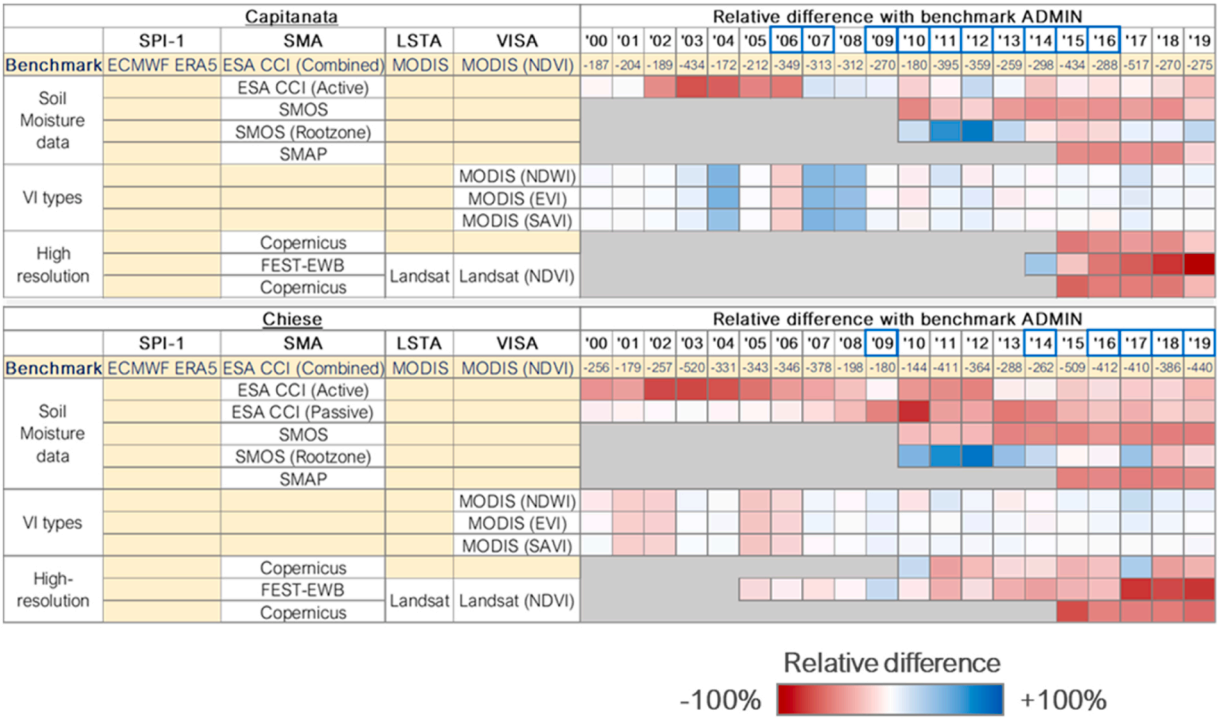

Fig. 11. Impact of different satellite products on ADMIN, for both Capitanata and Chiese case studies, for the years 2000–2019. Benchmark ADMIN is highlighted with a light-yellow background, and each row identifies a specific variation of the satellite product on a certain anomaly. The yearly ADMIN relative difference with the benchmark combination of products is represented by cell color, with years without data for comparison left in grey. Years with observed irrigation volumes data available are bordered in thick blue.

similarities with the ADMIN computed with ESA CCI Combined product (benchmark ADMIN), even though five years is too short a temporal horizon to provide absolute results.

Similarly, the impact of the four considered vegetation indices on the computation of the annual ADMIN is evaluated and it is generally very mild (Fig. 11), as a consequence of the high correlation among NDVI, NDWI, EVI and SAVI anomalies. This concept generally holds, except for some years (2004, 2007 and 2008) in the Capitanata area, when higher yearly ADMIN values are detected.

In the last rows of Fig. 11, a focus on high resolution is performed, featuring both high-resolution SM datasets (the 1 km Copernicus and the 30 m results from the FEST-EWB hydrological model) and LST and NDVI datasets (Landsat imagery instead of MODIS). Using higher-resolution datasets can limit the revisit time but might improve the representation of spatial heterogeneities in complex agricultural areas. For both Chiese and Capitanata, the second half of the years 2010 s records some negative differences in terms of ADMIN, with respect to the benchmark ADMIN. This effect is more marked in the Capitanata case study, as expected from a highly-heterogeneous area, with numerous empty plots bordering active agricultural fields. The differences are less marked in the Chiese case

Determination coefficient 0 1

					Capitanata						Chiese					
					v. Irrigation			v. Crop Yield			v. Irrigation			v. Crop Yield		
	SPI-1	SMA	LSTA	VISA	n	slope	R^2	n	slope	R^2	n	slope	R^2	n	slope	R^2
Benchmark	ECMWF ERA5	ESA CCI (Combined)	MODIS	MODIS (NDVI)	10	-0.06	0.18	14	-0.54	0.17	6	+1.13	0.26	14	+1.07	0.32
Soil Moisture data		ESA CCI (Active)			10	-0.05	0.14	14	-0.29	0.08	6	+3.54	0.41	14	+2.09	0.30
		ESA CCI (Passive)									6	+1.13	0.26	14	+1.94	0.35
		SMOS			7	-0.07	0.42	10	-0.60	0.18	5	*-0.67*	0.02	10	*-0.28*	0.00
		SMOS (Rootzone)			7	-0.03	0.51	10	-0.11	0.03	5	+0.69	0.49	10	+0.45	0.05
		SMAP			*2*	-	-	5	*+0.17*	0.31	4	*-3.69*	0.94	5	+0.36	0.00
VI types				MODIS (NDWI)	10	-0.01	0.01	14	-0.72	0.54	6	+1.38	0.28	14	+1.49	0.28
				MODIS (EVI)	10	-0.03	0.04	14	-0.14	0.06	6	+1.43	0.29	14	+1.74	0.29
				MODIS (SAVI)	10	-0.02	0.03	14	-0.21	0.05	6	+1.50	0.23	14	+1.65	0.25
High resolution		Copernicus			*2*	-	-	5	*+0.05*	0.12	5	+0.38	0.30	10	+1.78	0.35
		FEST-EWB	Landsat	Landsat (NDVI)	3	-0.00	0.01	6	-0.12	0.03	6	*-0.70*	0.13	14	+0.41	0.01
		Copernicus			*2*	-	-	5	*+0.01*	0.01	4	+4.47	0.45	5	*-3.15*	0.09

Fig. 12. Comparison between yearly ADMIN obtained from different satellite products, against irrigation volumes and final crop yield, for both Capitanata and Chiese case studies. Benchmark ADMIN is highlighted with a light-yellow background, and each row identifies a specific variation of the satellite product on a certain anomaly. For each comparison, the number of data points (n), the slope of the linear regression (slope) and the determination coefficient (R^2) are shown. Dependencies with a different sign than the one of the benchmark ADMIN are highlighted in red.

study, being quite close to zero in the 2005–2013 period (for the FEST-EWB + Landsat combination) and generally low when employing Copernicus SSM, as expected from an area more urbanized but definitely more homogeneous in terms of crop distribution.

Finally, the uncertainty of the ADMIN impact on the relationship with irrigation volumes and crop yields is computed, by considering the different combinations of the remotely sensed products for the different variables (Fig. 12). For both case studies, and for all the combinations described until now, the same comparisons as shown in Figs. 8 and 9 are performed, and the slope and determination coefficient of the linear interpolation are provided. The products for which only 2 datapoints are available are excluded from the analysis.

For the Capitanata case study, all combinations show a negative slope of the linear relationship between yearly ADMIN and cumulative irrigation, confirming how during drier years higher water volumes are employed; hence providing similar results to the benchmark ADMIN. The strength of these relationships is described by the determination coefficient, with the default ADMIN being in third place overall, but over a longer set of years than the top two combinations (powered by the two versions of SMOS). Looking at crop yields, the slopes of the linear relationship with yearly ADMINs are expected to be negative, as drier conditions (lower ADMIN values) are associated with less developed crops. This is the case for most combinations, except for the ADMINs employing SMAP or Copernicus as SSM source (although the strength of these relations is quite low and the datapoints available are too few to derive robust conclusions from this comparison).

In the Chiese area, on the other hand, irrigation is provided in a fixed pattern independently of the year dryness, and this is reflected in the linear relationships between irrigation and yearly ADMIN. The slopes of the different combinations are more heterogeneous in sign. As drought conditions and water volumes should be weakly correlated, the lowest determination coefficients mark generally better performances (e.g., those from SMOS and the benchmark ADMIN). Finally, looking at crop yields, the weakness of the linear relationships of the different combinations are justified by the large water amounts employed that smooth out the year-to-year variation in dry conditions. As seen for the comparisons between the different versions of ADMIN, the considerable heterogeneity of this agricultural area means that few major differences emerge in employing higher-resolution datasets.

5. Discussion and conclusion

Following the principles of the Common Agricultural Policy (CAP) to improve irrigation management to reduce crop damages and to enhance economic income, an EO-based drought indicator, ADMIN, has been developed for the operative management of irrigation networks, demonstrating its capability in providing reliable estimates of drought conditions correctly identifying the wet and dry years. The ADMIN might help irrigation districts managers and farmers to activate the preventive protection actions to try to avoid water volume and crop yield losses. The methodology has been applied in two cases studies: the Chiese and Capitanata Irrigation Consortia in Italy, over 20 years of analysis for the period from 2000 to 2019.

The robustness of the developed drought index has been evaluated by assessing the effect of drought events on the effectively used irrigation volumes and yearly crop yields at Irrigation Consortium Scale, in Southern and Northern Italy. This quantitative verification of the methodology, especially against irrigation volumes, represents an innovative point in respect to the generally implemented drought monitoring systems, mostly not validated with external data but relying only on comparisons among indices (Wood et al., 2015; Sheffield et al., 2012; van Dijk et al., 2013) or economic impacts evaluation (Ding et al., 2011). In the Capitanata Consortium, a negative correlation is obtained between the yearly cumulative drought index values and irrigation volumes, where an increase in the drought index means an increase of dryness condition, meaning that more irrigation is required; conversely in the Chiese Consortium a zero correlation is obtained with an almost constant amount of irrigation volumes provided to the crops every year independently from the drought condition. This might be explainable by the irrigation water payment plan, where in the Capitanata Irrigation Consortium the farmers pay a quota for m^3 of water used per ha, so that during wetter years, less irrigation volumes are provided; while in the Chiese Consortium, the farmers pay a fixed quota every year per ha independently from the volumes of water used, so during the rainy years, too much water is probably provided to the crops. In both analyzed areas, crop yields seem to be almost uncorrelated to the drought index, probably due to the fact that the area is highly irrigated during summer and that the amount of irrigation is capable of contrasting the drought conditions allowing to maintain an almost constant production over the years.

One of the strengths of the developed procedure relies on the capability of capturing the temporal evolution of the agricultural drought process, by firstly considering the meteorological drought and then the agricultural one, vegetation water stress and crop drying. This methodology improves the traditional analysis, which are generally analysed by considering only soil moisture anomalies (van Hateren et al., 2021; Sadri et al., 2018). In fact, the results of this work clearly show that asynchronies may exist especially between soil moisture anomalies and vegetation or land surface temperature anomalies, with negative SMA and positive VISA. This situation might be especially relevant when conditions of energy limited to vegetation growth are present, so that vegetation is less affected by soil moisture changes. This is due to the multifaced processes of vegetation, which is not driven only by water availability (Nemani et al., 2003; Jin et al., 2023).

These results are in general agreement with the findings of Wanders et al. (2017), Bachmair et al. (2018), Tijdeman et al. (2022), who highlighted that, generally, droughts cannot be described by one single indicator but there is the need first to select the correct physical index for detecting a drought type and secondly to use different drought indices to identify specific conditions to avoid disagreements among information sources (Parsons et al., 2019; Sheffield et al., 2012).

Another strength of the developed methodology is that the ADMIN is fully based on remote sensing data, considering different products of the same variable which differ on the sensing techniques, the spatial and temporal resolutions. The combinations of different products lead to different absolute drought values but these are almost all consistent (e.g. positive or negative anomalies). Given this, the ADMIN could be easily exported in any area worldwide.

In particular, seven to eight soil moisture products anomalies have been compared and generally low Pearson correlation values are found with a better correlation in the Chiese area, probably due to higher average yearly rainfalls which correspond with a more stable, less peaked SM behaviour, easier to reproduce from products working at different resolutions and with different algorithms. The results show how the ESA CCI datasets are the ones best correlated to each other overall, even if this result is mainly driven by the fact the ESA CCI Combined dataset includes the other two (Active and Passive). The reason why satellite SM does not show encouraging results may lie, among other reasons, in the fact that satellite soil moisture products are limited to the top few cm of soil, whereas a soil moisture drought assessment is ideally based on observations over the entire root zone, as well as the presence of coastlines in nearby the Capitanata area or the water bodies in the Chiese Consortium. The physical inconsistencies that satellite SSM data shows against water input (both rainfall and irrigation) make them not fully suitable to be used alone in drought detection.

On the other hand, high consistency has been obtained among different vegetation indices, with NDVI anomalies showing a high Pearson correlation especially with EVI and SAVI anomalies. This result in terms of anomalies confirms the general behaviour of this multitude of vegetation indices which, even if they produce slightly different results in terms of vegetation water status, does not significantly change the drought detection (Shahabfar et al., 2012).

Another point worth of notice is the insertion of the LST anomaly into the drought monitoring index to detect the plant water stress in advance in respect to plant drying. This relies on the fact that the LST is the driving factor of the partitioning between latent and sensible heat fluxes in the energy balance. This LST consideration is an improvement of the generally used agricultural drought indices, which are mostly based on rainfall, soil moisture or vegetation indices.

This paper tried to respond also the issues related to spatial resolution of satellite data answering to the question if high resolution information is needed for drought monitoring and irrigation aqueduct management. The obtained results indicate the advantage of using high-resolution data in respect to low resolution data, as being able to catch the same behavior in terms of agricultural drought detection at Irrigation district scale, and potentially offers important new advantages for applications even down to field scales. This might be particularly relevant in complex landscapes, where low resolution data might produce contrasting signals, leading to a limitation to the applicability of ADMIN

CRediT authorship contribution statement

Ahmad Al Bitar: Validation, Supervision, Methodology. **Nicola Paciolla:** Writing – original draft, Investigation, Formal analysis, Data curation. **Giada Restuccia:** Formal analysis, Data curation. **Chiara Corbari:** Writing – original draft, Validation, Supervision, Methodology, Formal analysis, Conceptualization.

Declaration of Competing Interest

The authors declare that they have no known competing financial interests or personal relationships that could have appeared to influence the work reported in this paper.

Data Availability

Data will be made available on request.

Acknowledgements

This work has been developed under the project: RET-SIF real time soil moisture forecast for smart irrigation (EU ERANETMED Programme) – 2018–2021 funded by the Italian Ministry of Education (MIUR). Hersbach, H. et al., (2018) was downloaded from the Copernicus Climate Change Service (C3S) Climate Data Store. The results contain modified Copernicus Climate Change Service information.

References

Abramowitz, M., Stegun, I.A., 1964. Handbook of Mathematical Functions with Formulas, Graphs, and Mathematical Tables. National Bureau of Standards, Applied Mathematics Series, p. 55.

AghaKouchak, A., Farahmand, A., Melton, F.S., Teixeira, J., Anderson, M.C., Wardlow, B.D., Hain, C.R., 2015. Remote sensing of drought: progress, challenges and opportunities. Geophys. Rev. https://doi.org/10.1002/2014RG000456.

Al Bitar, A., Kerr, Y.H., Cabot, F., Global drought index from SMOS soil moisture, Conference: IEEE International Geoscience and Remote Sensing Symposium, IGARSS 2013.

Al Bitar, A., Mialon, A., Kerr, Y.H., Cabot, F., Richaume, P., Jacquette, E., Quesney, A., Mahmoodi, A., Tarot, S., Parrens, M., et al., 2017. The global SMOS Level 3 daily soil moisture and brightness temperature maps. Earth Syst. Sci. Data 9, 293–315. https://doi.org/10.5194/essd-9-293-2017.

Alexandratos, N., Bruinsma, J., 2012. World agriculture towards 2030/2050: the 2012 revision. ESA Working paper No. 12-03. Rome, FAO.

Babaeian, E., Sadeghi, M., Jones, S.B., Montzka, C., Vereecken, H., Tuller, M., 2019. Ground, proximal, and satellite remote sensing of soil moisture. Rev. Geophys. 57, 530–616. https://doi.org/10.1029/2018RG000618.

Bachmair, S., Tanguy, M., Hannaford, J., Stahl, K., 2018. How well do meteorological indicators represent agricultural and forest drought across Europe? Environ. Res. Lett. 13 (3), 034042.

Bauer-Marschallinger, B., Paulik, C., Hochstöger, S., Mistelbauer, T., Modanesi, S., Ciabatta, L., Massari, C., Brocca, L., Wagner, W., 2018. Soil moisture from fusion of scatterometer and SAR: closing the scale gap with temporal filtering. Remote Sens 10, 1030. https://doi.org/10.3390/rs10071030.

Beck, H.E., Vergopolan, N., Pan, M., Levizzani, V., van Dijk, A.I.J.M., Weedon, G.P., Brocca, L., Pappenberger, F., Huffman, G.J., Wood, E.F., 2017. Global-scale evaluation of 22 precipitation datasets using gauge observations and hydrological modelling. Hydrol. Earth Syst. Sci. 21, 6201–6217. https://doi.org/10.5194/hess-21-6201-2017.

Bindlish, R., Barros, A.P., 2001. Parameterization of vegetation backscatter in radar-based, soil moisture estimation. Remote Sens. Environ. 76 (1), 130–137.

Blauhut, V., Stephan, R., Stahl, K., 2022. The European Drought Impact Report Inventory (EDII V2.0). Version 2.0. ⟨https://doi.org/10.6094/UNIFR/230922⟩.

Cammalleri, C., Arias-Muñoz, C., Barbosa, P., de Jager, A., Magni, D., Masante, D., Mazzeschi, M., McCormick, N., Naumann, G., Spinoni, J., Vogt, J., 2021. A revision of the Combined Drought Indicator (CDI) used in the European Drought Observatory (EDO). Nat. Hazards Earth Syst. Sci. 21, 481–495. https://doi.org/10.5194/nhess-21-481-2021.

Choudhury, B.J., 1987. Relationships between vegetation indices, radiation absorption, and net photosynthesis evaluated by a sensitivity analysis. Remote Sens. Environ. 22, 209–233. https://doi.org/10.1016/0034-4257(87)90059-9.

Coldiretti, 2017. ⟨https://www.coldiretti.it/ambiente-e-sviluppo-sostenibile/ispra-ora-siccita-peggiore-nel-2017⟩.

Corbari, C., Mancini, M., 2022. Irrigation efficiency optimization at multiple stakeholders' levels based on remote sensing data and energy water balance modelling, 1432-1319 Irrig. Sci.. https://doi.org/10.1007/s00271-022-00780-4.

Crow, W.T., Berg, A.A., Cosh, M.H., Loew, A., Mohanty, B.P., Panciera, R., de Rosnay, P., Ryu, D., Walker, J.P., 2012. Upscaling sparse ground-based soil moisture observations for the validation of coarse-resolution satellite soil moisture products. L19406 Rev. Geophys. 50, 2011RG000372. https://doi.org/10.1029/2011RG000372.

Cui, C., Xu, J., Zeng, J., Chen, K.-S., Bai, X., Lu, H., Chen, Q., Zhao, T., 2017. Soil Moisture Mapping from Satellites: An Intercomparison of SMAP, SMOS, FY3B, AMSR2, and ESA CCI over Two dense network regions at different spatial scales. Remote Sens 10, 33.

De Stefano, L., Fornés, J.M., López-Geta, J.A., Villarroya, F., 2015. Groundwater use in Spain: an overview in light of the EU water framework directive. Int. J. Water Resour. Dev. 31 (4), 640–656. https://doi.org/10.1080/07900627.2014.938260.

Ding, Y., Hayes, M.J., Widhalm, M., 2011. Measuring economic impacts of drought: a review and discussion. Disaster Prev. Manag. 20, 434–446. https://doi.org/10.1108/09653561111161752.

Diodato, N., Bellocchi, G., 2008. Drought stress patterns in Italy using agro-climatic indicators. Clim. Res. 36, 53–63. https://doi.org/10.1007/10.3354/cr00726.

Dorigo, W., Wagner, W., Albergel, C., Albrecht, F., Balsamo, G., Brocca, L., Chung, D., Ertl, M., Forkel, M., Gruber, A., et al., 2017. ESA CCI Soil moisture for improved earth system understanding: state-of-the art and future directions. Remote Sens. Environ. 203, 185–215. https://doi.org/10.1016/j.rse.2017.07.001.

Douville, H., Raghavan, K., Renwick, J., Allan, R.P., Arias, P.A., Barlow, M., Cerezo-Mota, R., Cherchi, A., Gan, T.Y., Gergis, J., Jiang, D., Khan, A., Pokam Mba, W., Rosenfeld, D., Tierney, J., Zolina, O., 2021. Water Cycle Changes. In: Zhai, V., P., Pirani, A., Connors, S.L., Péan, C., Berger, S., Caud, N., Chen, Y., Goldfarb, L., Gomis, M.I., Huang, M., Leitzell, K., Lonnoy, E., Matthews, J.B.R., Maycock, T.K., Waterfield, T., Yelekçi, O., Yu, R., Zhou, B. (Eds.), Climate Change 2021: The Physical Science Basis. Contribution of Working Group I to the Sixth Assessment Report of the Intergovernmental Panel on Climate Change [Masson-Delmotte. Cambridge University Press,, Cambridge, United Kingdom and New York, NY, USA, pp. 1055–1210. https://doi.org/10.1017/9781009157896.010.

Duan, S.-B., Li, Z.-L., Li, H., Göttsche, F.M., Wu, H., Zhao, W., Leng, P., Zhang, X., Coll, C., 2019. Validation of Collection 6 MODIS land surface temperature product using in situ measurements. Remote Sens. Environ. 225, 16–29. https://doi.org/10.1016/j.rse.2019.02.020.

EDO) 2020 EDO Indicator factsheet—standardized precipitation index (SPI) (Copernicus European Drought Observatory (EDO)) 1–5 (available at: ⟨https://edo.jrc.ec.europa.eu/⟩).

El Hajj, M., Baghdadi, N., Zribi, M., Rodríguez-Fernández, N., Wigneron, J.P., Al-Yaari, A., Al Bitar, A., Albergel, C., Calvet, J.-C., 2018. Evaluation of SMOS, SMAP, ASCAT and Sentinel-1 Soil Moisture Products at Sites in Southwestern France. Remote Sens 10, 569. https://doi.org/10.3390/rs10040569.

Entekhabi, D., Yueh, S., O'Neill, P.E., Kellogg, K.H., Allen, A., Bindlish, R., Johnson, J., 2014. In: SMAP Handbook—Soil Moisture Active Passive—Mapping Soil Moisture and Freeze/Thaw from Space. JPL Publication, Pasadena, CA, USA, pp. 400–1567.

Famiglietti, J.S., Ryu, D.R., Berg, A.A., Rodell, M., Jackson, T.J., 2008. Field observations of soil moisture variability across scales. Water Resour. Res. 44, W01423. https://doi.org/10.1029/2006WR005804.

FAO). Global Map of Irrigation Areas (GMIA). ⟨http://www.fao.org/nr/water/aquastat/irrigationmap/index.stm⟩ (2016).

Gao, B.-C., 1996. NDWI—A normalized difference water index for remote sensing of vegetation liquid water from space. Remote Sens. Environ. 58 (3), 257–266. https://doi.org/10.1016/S0034-4257(96)00067-3.

García-Herrera, R., Díaz, J., Trigo, R.M., Luterbacher, J., Fischer, E.M., 2010. A Review of the European Summer Heat Wave of 2003. Crit. Rev. Environ. Sci. Technol. 40 (4), 267–306. https://doi.org/10.1080/10643380802238137.

Giacomelli, A., Bacchiega, U., Troch, P.A., Mancini, M., 1995. Evaluation of surface soil moisture distribution by means of SAR remote sensing techniques and conceptual hydrological modelling. J. Hydrol. 166, 445–459. https://doi.org/10.1016/0022-1694(94)05100-C.

Gruber, A., Scanlon, T., Van Der Schalie, R., Wagner, W., Dorigo, W., 2019. Evolution of the ESA CCI Soil Moisture climate data records and their underlying merging methodology. Earth Syst. Sci. Data 11, 717–739. https://doi.org/10.5194/essd-11-717-2019.

Gu, Y., Hunt, E., Wardlow, B., Basara, J.B., Brown, J.F., Verdin, J.P., 2008. Evaluation of MODIS NDVI and NDWI for vegetation drought monitoring using Oklahoma Mesonet soil moisture data. Geophys. Res. Lett. 35, L22401. https://doi.org/10.1029/2008GL035772.

Hersbach, H., Bell, B., Berrisford, P., Biavati, G., Horányi, A., Muñoz Sabater, J., Nicolas, J., Peubey, C., Radu, R., Rozum, I., Schepers, D., Simmons, A., Soci, C., Dee, D., Thépaut, J.-N., 2018. ERA5 hourly data on single levels from 1959 to present. Copernicus Climate Change Service (C3S) Climate Data Store (CDS). (Accessed on 12-April-2020).

Hersbach, H., Bell, B., Berrisford, P., Hirahara, S., Horányi, A., Muñoz-Sabater, J., Nicolas, J., Peubey, C., Radu, R., Schepers, D., Simmons, A., Soci, C., Abdalla, S., Abellan, X., Balsamo, G., Bechtold, P., Biavati, G., Bidlot, J., Bonavita, M., Chiara, G., Dahlgren, P., Dee, D., Diamantakis, M., Dragani, R., Flemming, J., Forbes, R., Fuentes, M., Geer, A., Haimberger, L., Healy, S., Hogan, R.J., Hólm, E., Janisková, M., Keeley, S., Laloyaux, P., Lopez, P., Lupu, C., Radnoti, G., Rosnay, P., Rozum, I., Vamborg, F., Villaume, S., Thépaut, J.N., 2020. The ERA5 global reanalysis. Q. J. R. Meteorol. Soc. 146 (730), 1999–2049.

Hoffmann, D., Gallant, A.J.E., Arblaster, J.M., 2020. Uncertainties in Drought From Index and Data Selection. JGR Atmos. 125 (18) https://doi.org/10.1029/2019JD031946.

Huang, S., Chang, J., Leng, G., Huang, Q., 2015. Integrated index for drought assessment based on variable fuzzy set theory: a case study in the Yellow River basin, China. J. Hydrol. 527, 608–618.

Huete, A.R., 1988. A Soil-Adjusted Vegetation Index (SAVI). Remote Sens. Environ. 25, 295–309. https://doi.org/10.1016/0034-4257(88)90106-x.

Huete, A.R., Liu, H.Q., Batchily, K.V., Van Leeuwen, W.J.D.A., 1997. A comparison of vegetation indices over a global set of TM images for EOS-MODIS. Remote Sens. Environ. 59 (3), 440–451.

Jiménez-Donaire, M.P., Tarquis, A., Giráldez, J.V., 2020. Evaluation of a combined drought indicator and its potential for agricultural drought prediction in southern Spain. Nat. Hazards Earth Syst. Sci. 20, 21–33. https://doi.org/10.5194/nhess-20-21-2020.

Jimenez-Munoz, J.C., Sobrino, J.A., Skokovic, D., Mattar, C., Cristobal, J., 2014. Land surface temperature retrieval methods from landsat-8 thermal infrared sensor data. IEEE Geosci. Remote Sens. Lett. 11, 1840–1843.

Jin, H., Vicente-Serrano, S.M., Tian, F., et al., 2023. Higher vegetation sensitivity to meteorological drought in autumn than spring across European biomes. Commun. Earth Environ. 4, 299. https://doi.org/10.1038/s43247-023-00960-w.

Kerr, Y.H., Waldteufel, P., Wigneron, J.-P., Delwart, S., Cabot, F., Boutin, J., Escorihuela, M.-J., Font, J., Reul, N., Gruhier, C., et al., 2010. The SMOS mission: new tool for monitoring key elements of the global water cycle. Proc. IEEE 98, 666–687. https://doi.org/10.1109/jproc.2010.2043032.

Kogan, Felix N., 1997. Global drought watch from space. Bull. Am. Meteorol. Soc. 78 (4), 621–636. https://doi.org/10.1175/1520-0477(1997)078<0621:GDWFS>2.0.CO;2.

Komuscu, A.U., 1999. Using the SPI to analyze spatial and temporal patterns of drought in Turkey. Drought Netw. N. 11 (1), 7–13.

Kumar, R., Musuuza, J.L., Van Loon, A.F., Teuling, A.J., Barthel, R., Ten Broek, J., Attinger, S., et al., 2016. Multiscale evaluation of the Standardized Precipitation Index as a groundwater drought indicator. Hydrol. Earth Syst. Sci. 20 (3), 1117–1131.

Kustas, W.P., Norman, J.M., 1999. Evaluation of soil and vegetation heat flux predictions using a simple two-source model with radiometric temperatures for partial canopy cover. Agric. For. Meteor. 94, 13–29. https://doi.org/10.1016/S0168-1923(99)00005-2.
Leeper, R.D., Bilotta, R., Petersen, B., Stiles, C.J., Heim, R., Fuchs, B., Prat, O.P., Palecki, M., Ansari, S., 2022. Characterizing U.S. drought over the past 20 years using the U.S. drought monitor. Int. J. Climatol. 42 (12), 6616–6630. https://doi.org/10.1002/joc.7653.
Liu, H.Q., Huete, A., 1995. Feedback based modification of the NDVI to minimize canopy background and atmospheric noise. IEEE Trans. Geosci. Remote Sens. 33 (2), 457–465.
Luan, Qingzu, et al., 2015. An integrated service system for agricultural drought monitoring and forecasting and irrigation amount forecasting. 2015 23rd International Conference on Geoinformatics. IEEE,.
Mann, M.E., Gleick, P.H., 2015. Climate change and California drought in the 21st century. P. Natl. Acad. Sci. USA 112, 3858–3859.
McKee, T.B., Doesken, N.J., Kleist, J., 1993. The relationship of drought frequency and duration to time scale. Proceedings of the Eighth Conference on Applied Climatology, Anaheim, California. American Meteorological Society,, Boston, pp. 179–184.
McKee, T.B., Doesken, N.J., Kleist, J., 1995. Drought monitoring with multiple time scales. Proc. Ninth Conf. Appl. Climatol. 233–236.
Meza, I., Rezaei, E.E., Siebert, S., Ghazaryan, G., Nouri, H., Dubovyk, O., Hagenlocher, M., et al., 2021. Drought risk for agricultural systems in South Africa: Drivers, spatial patterns, and implications for drought risk management. Sci. Total Environ. 799, 149505 https://doi.org/10.1016/j.scitotenv.2021.149505.
Miralles, D.G., Gentine, P., Seneviratne, S.I., Teuling, A.J., 2019. Land–atmospheric feedbacks during droughts and heatwaves: state of the science and current challenges. Ann. N. Y. Acad. Sci. 1436, 19–35. https://doi.org/10.1111/nyas.13912.
Musolino, D., Vezzani, C. and Massarutto, A., 2018. Drought Management in the Po River Basin, Italy. In Drought (eds A. Iglesias, D. Assimacopoulos and H.A. Van Lanen). ⟨https://doi.org/10.1002/9781119017073.ch11⟩.
Nemani, R.R., Keeling, C.D., Hashimoto, H., Jolly, W.M., Piper, S.C., Tucker, C.J., Myneni, R.B., Running, S.W., 2003. Climate-driven increases in global terrestrial net primary productivity from 1982 to 1999. Science 300, 1560–1563.
Ozelkan, Emre, Chen, Gang, Ustundag, Burak Berk, 2016. Multiscale object-based drought monitoring and comparison in rainfed and irrigated agriculture from Landsat 8 OLI imagery. Int. J. Appl. Earth Obs. Geoinf. 44, 159–170.
Paciolla, N., Corbari, C., Al Bitar, A., Kerr, Y., Mancini, M., 2020. Irrigation and Precipitation Hydrological Consistency with SMOS, SMAP, ESA-CCI, Copernicus SSM1km, and AMSR-2 Remotely Sensed Soil Moisture Products. Remote Sens 12, 3737. https://doi.org/10.3390/rs12223737.
Parsons, D.J., Rey, D., Tanguy, M., Holman, I.P., 2019. Regional variations in the link between drought indices and reported agricultural impacts of drought. Agric. Syst. 173, 119–129.
Price, J.C., 1980. The potential of remotely sensed thermal infrared data to infer surface soil moisture and evaporation. Water Resour. Res. 16 (4), 787–795. https://doi.org/10.1029/WR016i004p00787.
Sadri, S., Wood, E.F., Pan, M., 2018. Developing a drought-monitoring index for the contiguous US using SMAP. Hydrol. Earth Syst. Sci. 22, 6611–6626. https://doi.org/10.5194/hess-22-6611-2018.
Seneviratne, S.I., Zhang, X., Adnan, M., Badi, W., Dereczynski, C., Di Luca, A., Ghosh, S., Iskandar, I., Kossin, J., Lewis, S., Otto, F., Pinto, I., Satoh, M., Vicente-Serrano, S.M., Wehner, M., Zhou, B., 2021. Weather and Climate Extreme Events in a Changing Climate. In: Masson-Delmotte, V., Zhai, P., Pirani, A., Connors, S. L., Péan, C., Berger, S., Caud, N., Chen, Y., Goldfarb, L., Gomis, M.I., Huang, M., Leitzell, K., Lonnoy, E., Matthews, J.B.R., Maycock, T.K., Waterfield, T., Yelekçi, O., Yu, R., Zhou, B. (Eds.), Climate Change 2021: The Physical Science Basis. Contribution of Working Group I to the Sixth Assessment Report of the Intergovernmental Panel on Climate Change. Cambridge University Press,, Cambridge, United Kingdom and New York, NY, USA, pp. 1513–1766. https://doi.org/10.1017/9781009157896.013.
Sepulcre-Canto, G., Horion, S.M.A.F., Singleton, A., Carrao, H., Vogt, J., 2012. Development of a Combined Drought Indicator to detect agricultural drought in Europe. Nat. Hazards Earth Syst. Sci. 12 (11), 3519–3531.
Shahabfar, A., Ghulam, A., Eitzinger, J., 2012. Drought monitoring in Iran using the perpendicular drought indices. Int. J. Appl. Earth Obs. Geoinf. 18, 119–127. https://doi.org/10.1016/j.jag.2012.01.011.
Sheffield, J., Andreadis, K.M., Wood, E.F., Lettenmaier, D.P., 2009. Global and continental drought in the second half of the twentieth century: Severity–area–duration analysis and temporal variability of large-scale events. J. Clim. 22 (8), 1962–1981. https://doi.org/10.1175/2008JCLI2722.1.
Sheffield, J., Wood, E.F., Roderick, M.L., 2012. Little change in global drought over the past 60 years. Nature 491 (7424), 435–438.
Sheffield, J., Wood, E.F., Chaney, N., Guan, K., Sadri, S., Yuan, X., Olang, L., Amani, A., Ali, A., Demuth, S., 2014. A Drought Monitoring and Forecasting System for Sub-Sahara African Water Resources and Food Security. B. Am. Meteorol. Soc. 95, 861–882.
Shyrokaya, A., Messori, G., Pechlivanidis, I., Pappenberger, F., Cloke, H.L., Di Baldassarre, G. (Eds.), 2024. Significant relationships between drought indicators and impacts for the 2018-2019 drought in Germany. Environ. Res. Lett. 19, 014037.
Spinoni, J., Vogt, J.V., Naumann, G., Barbosa, P., Dosio, A., 2018. Will drought events become more frequent and severe in Europe? Int J. Clim. 38 (4), 1718–1736.
Su, Z., 2002. The Surface Energy Balance System (SEBS) for estimation of turbulent heat fluxes. Hydrol. Earth Syst. Sci. 6, 85–100. https://doi.org/10.5194/hess-6-85-2002.
Swain, D.L., Tsiang, M., Haugen, M., Singh, D., Charland, A., Rajaratnam, B., Diffenbaugh, N.S., 2014. The extraordinary California drought of 2013/2014: character, context, and the role of climate change. Bull. Am. Meteorol. Soc. 95, S3–S7.
Thom, H.C.S., 1958. A Note on the Gamma Distribution. Mon. Weather Rev. 86 (4).
Tijdeman, E., Blauhut, V., Stoelzle, M., Menzel, L., Stahl, K., 2022. Different drought types and the spatial variability in their hazard, impact, and propagation characteristics. Nat. Hazards Earth Syst. Sci. 22, 2099–2116. https://doi.org/10.5194/nhess-22-2099-2022.
van Dijk, A.I.J.M., Beck, H.E., Crosbie, R.S., de Jeu, R.A.M., Liu, Y.Y., Podger, G.M., Timbal, B., Viney, N.R., 2013. The Millennium Drought in southeast Australia (2001–2009): Natural and human causes and implications for water resources, ecosystems, economy, and society. Water Resour. Res. 49 https://doi.org/10.1002/wrcr.20123.
van Hateren, T.C., Chini, M., Matgen, P., Teuling, A.J., 2021. Ambiguous Agricultural Drought: Characterising Soil Moisture and Vegetation Droughts in Europe from Earth Observation. Remote Sens 13, 1990. https://doi.org/10.3390/rs13101990.
Van Loon, A.F., Tijdeman, E., Wanders, N., Van Lanen, H.A.J., Teuling, A.J., Uijlenhoet, R., 2014. How climate seasonality modifies drought duration and deficit. J. Geophys. Res. -Atmos. 119, 4640–4656. https://doi.org/10.1002/2013JD020383.
Vicente-Serrano, S.M., 2006. Differences in spatial patterns of drought on different time scales: An analysis of the Iberian Peninsula. Water Resour. Manag. 20 (1), 37–60. https://doi.org/10.1007/s11269-006-2974-8.
Vicente-Serrano, S.M., Beguería, S., López-Moreno, J.I., 2010. A multiscalar drought index sensitive to global warming: the standardized precipitation evapotranspiration index. J. Clim. 23 (7), 1696–1718.
Vogt, J., Naumann, G., Masante, D., Spinoni, J., Cammalleri, C., Erian, W., Barbosa, P., 2018. Drought risk assessment and management. A Concept. Framew.
Wan, Z., 2008. New refinements and validation of the MODIS Land-Surface Temperature/Emissivity products. Remote Sens. Environ. 112, 59–74.
Wanders, N., Van Loon, A.F., Van Lanen, H.A.J., 2017. Frequently used drought indices reflect different drought conditions on global scale. Hydrol. Earth Syst. Sci. Discuss. https://doi.org/10.5194/hess-2017-512.
Wang, H., He, S., 2015. The north China/northeastern Asia severe summer drought in 2014. J. Clim. 28 (17), 6667–6681.
Wilhite, D.A., Glantz, M.H., 1985. Understanding the drought phenomenon: the role of definitions. Water Int 10 (3), 111–120. https://doi.org/10.1080/02508068508686328.
WMO) and Global Water Partnership (GWP), 2016: Handbook of Drought Indicators and Indices (M. Svoboda and B.A. Fuchs). Integrated Drought Management Programme (IDMP), Integrated Drought Management Tools and Guidelines Series 2. Geneva.
Wood, E.F., Schubert, S.D., Wood, A.W., Peters-Lidard, C.D., Mo, K.C., Mariotti, A., Pulwarty, R.S., 2015. Prospects for advancing drought understanding, monitoring, and prediction. J. Hydrometeorol. 16 (4), 1636–1657. https://doi.org/10.1175/JHM-D-14-0164.1.
World Meteorological Organization, 2012: Standardized Precipitation Index User Guide (M. Svoboda, M. Hayes and D. Wood). (WMO-No. 1090), Geneva.

Wu, Di, Qu, John J., Hao, Xianjun, 2015. Agricultural drought monitoring using MODIS-based drought indices over the USA Corn Belt. Int. J. Remote Sens. 36 (21), 5403–5425.

Wu, H., Svoboda, M.D., Hayes, M.J., Wilhite, D.A., Wen, F., 2007. Appropriate application of the standardized precipitation index in arid locations and dry seasons. Int J. Clim.: A J. R. Meteorol. Soc. 27 (1), 65–79.

Xue, J., Su, B., 2017. Significant remote sensing vegetation indices: a review of developments and applications. J. Sens. 17, 1353691 https://doi.org/10.1155/2017/1353691.